

APPROVED:

“ ___ ” May 2019

JINR Director V. Matveev

PROJECT

**DESIGN OF THE SC230 SUPERCONDUCTING CYCLOTRON FOR PROTON THERAPY
(91.5MHZ)**

Participants from JINR:

K. Bunyatov, S. Gurskiy, S. Fedorenko, I. Ivanenko, O. Karamyshev, G. Karamysheva, I. Kiyan,
V. Malinin, D. Popov, G. Shirkov, S. Shirkov, V. Smirnov, S. Vorozhtsov

Project Leader

G. Shirkov

Principal Conceptual Leader

O. Karamyshev

Division Leader

G. Karamysheva

JINR – ASIPP Collaboration

DUBNA, May 2019

Contents

Introduction	3
1. Magnet system of cyclotron SC-230	6
Iron material	6
Computer simulations of the magnet	8
Magnetostatic forces exerted on SC230 magnet	10
2. Equilibrium Orbit Calculation	14
3. Preliminary Beam dynamics estimations	17
5. Accelerating system design	20
Computer model	20
Power losses.	24
6. Beam dynamics analysis in SC230 cyclotron	24
Central region	27
Extraction system.....	32
Electrostatic deflector	36
Magnetic channels	37
Compensator.....	38
7. Magnetic field mapping system based on inductive coil	40
8. Vacuum System	44
Conclusion	45
Referencies	45
9. Project Technical schedule	47
10. Total estimated cost for the project	48
11 .Equipment summary	49
. Annex 1	51
Estimated cost for cyclotron parts to be purchased by ASIPP	

Abstract

Physical design of the compact superconducting cyclotron SC230 (91.5MHz) was performed. The cyclotron will deliver >230 MeV beam for proton therapy and research. We have performed simulations of magnetic and accelerating systems of the SC230 cyclotron and specified the main parameters of the accelerator. Possible schema of the extraction system and results of beam dynamicssimulations are presented.

INTRODUCTION

Since 2016 the SC200 superconducting cyclotron for hadron therapy has been jointly developed by JINR and ASIPP (Hefei, China) [1]. The production of the cyclotron faced a lot of engineering challenges which are mainly aroused due to high magnetic field of the accelerator. Therefore we decide to rethink some design decisions after careful analysis of SC200, other projects and operating cyclotrons for proton therapy.

Modern tendency to reduce size and cost of Ion Beam Radiotherapy leads to the success of superconducting synchrocyclotrons, which are useful for single room solutions. An isochronous cyclotron cannot compete with synchrocyclotrons in dimensions and weight, Mevion 250 weights about 20 tonnes [2], but a cyclotron has a CW beam and therefore high average current sufficient for different applications. The isochronous cyclotron is the best choice for the universal full-scale proton therapy centers.

Most proton therapy centers commissioned worldwide utilise isochronous cyclotrons as the drive accelerator, because they are compact, simple to operate and very reliable. Cyclotrons deliver a continuous output (CW beam) with high beam current and can accurately modulate the proton beam current.

Recent developments of superconducting cyclotrons for proton therapy, such as SC200, Pronova K230, Sumitomo 230MeV share similar parameters that define the structure of the cyclotron. All projects are 4-sector cyclotrons with ~3T central field. Such parameters were chosen in pursuit of compact dimensions. None of those cyclotrons are yet in operation.

There are two most successful accelerators in the proton therapy: Varian Proscan [3], design proposal by H.Blosser et al in 1993, and C235 (IBA Belgian) [4] (see Table 1). Both cyclotrons have much smaller central field, 2.4 and 1.7 Tesla.

Table 1. Comparison of parameters of cyclotrons for proton therapy

	MevionS250	Varian Proscan	IBAC235	SC230_91.5MHz
DYoke, m	1.8	3.1	4.34	4
Height, m	1	1.6	2.1	1.7
B ₀ , T	8.9	2.4	1.7	1.5
Coil	Nb ₃ Sn	NbTi	Resistive	NbTi or HTS?
Weight, tonnes	20	90	210	130
Beam time structure	Pulsed	CW	CW	CW
Extraction energy, MeV	250	250	235	230

We are not restricted in dimensions of cyclotron; therefore, we decided first of all to increase the pole of the cyclotron in order to decrease mean magnetic field to about 1.5 T in the center. Corresponding frequency for this value of the magnetic field is 91.5 MHz which was used for SC200 cyclotron design.

As the cyclotron will have a relatively small magnet field, it is possible to use both superconducting and resistive coil. Both solutions have their pros and cons, however for the SC230 we have chosen superconducting coil. Although the resistive coil is cheaper and easier, it consumes more power, it is a source of heat that may affect the cyclotron, and as we need 170kA-turns it would be large, and large resistive coil requires a rather complicated and powerful cooling system. For example, the resistive coil of the IBA C235 cyclotron, which delivers 250kA-turns is about 0.6x0.5m in cross-section, and superconducting coil with cryostat would be less than 0.25x0.25m. Our simulations show that similar design as IBA C235 with superconducting coil instead of copper coil would reduce the yoke weight from 210tonnes down to about 100tonnes and would make the cyclotron much more compact. Since in this proposal we reduce RF frequency even more than the frequency in C235, the accelerator weight will be about 130 tonnes.

The superconducting technologies are evolving and become more and more affordable, so running cost of the SC coil should decrease; however the same cannot be said about electricity costs, that is why we are focused on low power consumption of the cyclotron.

Low magnetic field is also an advantage for the SC coil design. The magnetic field in the coil is an important value, and critical current strongly depends on it. The usual value of the current density in NbTi coils in superconducting cyclotrons or synchrocyclotrons for proton therapy is 50-60A/mm², however, those coils operate at 4T and more, the SC230 coil will operate at 2T field in coil, and that can theoretically give us an order of magnitude greater possible current density and

reduce the coil size down to 10cm² and lower. But our focus is on reliability and simplicity and we prefer not to have risks of quench, so we plan to keep the current density moderate and it should not exceed 110A/mm².

Some data helpful to determine coil parameters:

Coil Max B = 2 T Critical current could be 10 times more than in SC200 where Bmax = 5 T;

Vertical Force between coils is about 1 tonne. In SC200 it is 100 tonne.

We plan to use NbTi for coil manufacture; however, the cyclotron's design makes it possible to use high-temperature superconductor (HTS) materials, which is very promising [5]. So far the liquid nitrogen temperature superconductors were very expensive and coil was manufactured only in short pieces of wire, not exceeding 1km. According to our calculations, we would need about 5km of wire. We are researching the possibility of using HTS because HTS materials provide large margin against quenching, need lower cryocoolers power and have more compact cryostat dimensions.

We propose a design which combines advantages of both successful accelerators: low magnetic field level and fourth harmonic of acceleration (C235 cyclotron), four accelerating cavities and superconducting coils (Varian PROSCAN).

As a result, we will have a design with:

- Minimum engineering efforts and challenges;
- Low power consumption (running costs should be low);
- High quality of the beam (regarded as the main feature);
- Reasonable size;
- Reliability and stable operation;
- Moderate conservativeness and reduced risks.

Table 2. Parameters of the cyclotron

Accelerated particles	protons
Magnet type	Compact, SC coil, warm yoke
Number of sectors	4
Number of RF cavities	4
Ion source	Internal, PIG
Final energy, MeV	>230
Number of turns	600

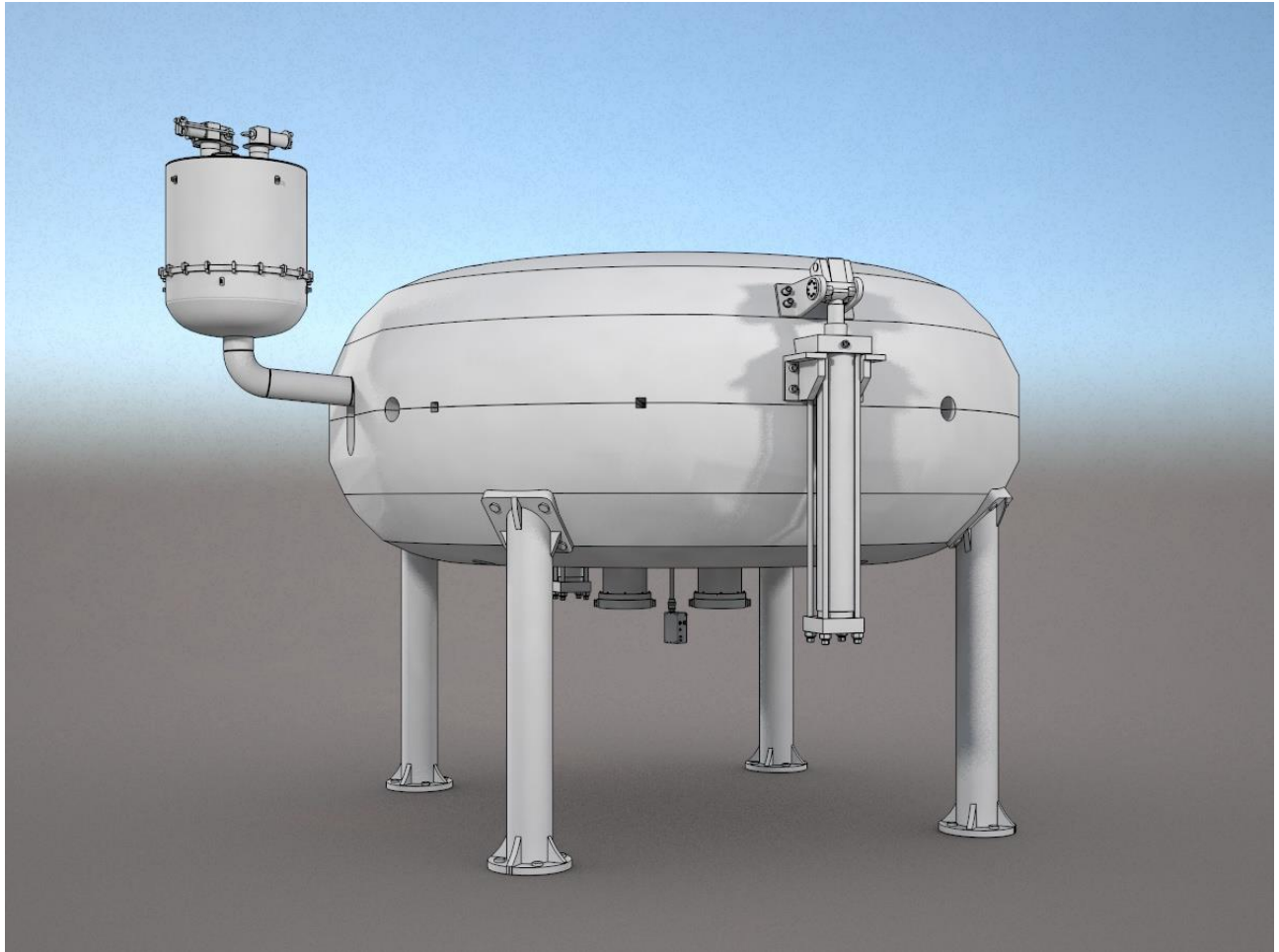


Figure 1: Overall view of the SC230 cyclotron

1. MAGNET SYSTEM OF CYCLOTRON SC-230

Iron material

Carbon steel chemical elements and mechanical properties for the SC230 can be the same as for SC202. The chemical components of steel 1010 for Chinese standard are collected in the Table 3. Some mechanical properties of steel 1010 also are given in Table 4.

Table 3. Carbon steel chemical elements for the SC230 (%)

components	GB standard	C	Si	Mn	Cr	Ni	Cu	S	P
Sectors, Yokes, Discs	Steel 1010	<u>0.07-0.09</u>	In the range of standard	In the range of standard	≤0.08	≤0.08	≤0.2 5	≤0.0 2	≤0.02 5

*refer to Chinese standard: GB/T699-1999

Table 4. Mechanical Properties for steel1010 for Chinese standard: **GB/T699-1999**

Num.	name	Heat treatment, °C	Mechanical property			
			σ_b MPa	σ_s MPa	δ_5 %	ψ %
1	Steel 1010	930	335	205	31	55

The measured B-H curve of steel product should be satisfied that of steel 1010 (see in theTable 5).

Table 5. Steel 1010

Hcp,kA/m	B,T	$\mu_0 M, T$	μ
1.260973	1.41168	1.410096	891.3031
1.692412	1.491634	1.489507	701.4703
2.484	1.566077	1.562956	501.7264
3.19331	1.609882	1.605869	401.2027
3.990113	1.645059	1.640045	328.0975
4.817673	1.675383	1.669329	276.7434
5.650749	1.702546	1.695445	239.7665
6.54238	1.72622	1.717999	209.9674
7.422785	1.748955	1.739627	187.5045
8.31027	1.767699	1.757256	169.2717
9.214061	1.786528	1.774949	154.2948
10.11977	1.803021	1.790305	141.782
11.25928	1.826637	1.812488	129.103
12.15611	1.840829	1.825553	120.5062
13.11735	1.857057	1.840573	112.66
14.03144	1.871257	1.853625	106.1263
15.9392	1.896773	1.876744	94.69778
19.09311	1.936618	1.912625	80.71564
24.10124	1.991051	1.960764	65.74053
29.2434	2.034837	1.998088	55.37219
34.80495	2.068981	2.025244	47.30487
40.67176	2.095538	2.044428	41.00085
52.51166	2.126849	2.060861	32.23081
64.70372	2.150417	2.069108	26.44744
76.37625	2.167828	2.071851	22.5869
87.99388	2.185256	2.07468	19.76242
99.48269	2.19984	2.074826	17.5968
128.2697	2.237849	2.076661	13.88344
156.6734	2.275817	2.078935	11.55932
184.1991	2.310449	2.078978	9.981575
211.6992	2.345281	2.079252	8.815887
255.2098	2.399563	2.078857	7.482125
298.7003	2.454779	2.079421	6.539837
318.9582	2.48004	2.079225	6.187498
344.9462	2.512128	2.078656	5.795363
369.2214	2.542469	2.078492	5.479729

394.673	2.574477	2.078516	5.19089
417.9272	2.603607	2.078424	4.957525
465.125	2.66331	2.078817	4.556615
509.0262	2.718335	2.078674	4.249648
548.8721	2.767942	2.078209	4.013063
588.6944	2.818327	2.078552	3.809707
626.3518	2.866029	2.078932	3.641266
659.5054	2.893021	2.078665	3.508166

Computer simulations of the magnet

Simulations were performed in CST studio[6] in the parametrized model of the magnet (see Figure 2) created in Autodesk Fusion 360 [7]. Changing parameters automatically changes the computer model. In addition, sector geometry can be replaced by importing from Matlab. Final cross check was performed with Tosca code.

The dimensions of the yoke (see Table 7 and Figure 3) were chosen to restrict the magnetic stray field in the range of 200-300G just outside accelerator, providing full saturation of the iron poles and yoke. Average magnetic field and flutter from CST simulation are presented in Figure 4. Low number harmonics for the model without magnetic channels are presented in Figure 5.

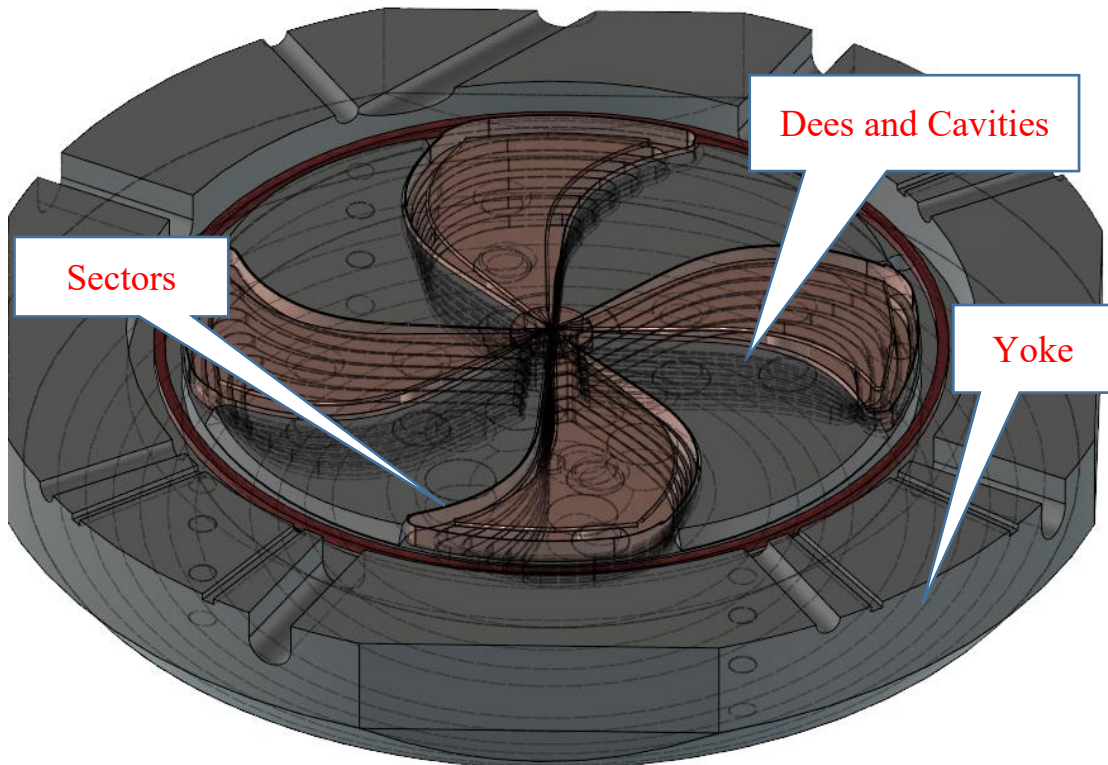


Figure 2: Layout of the cyclotron’s 3D computer model (magnet and accelerating system).

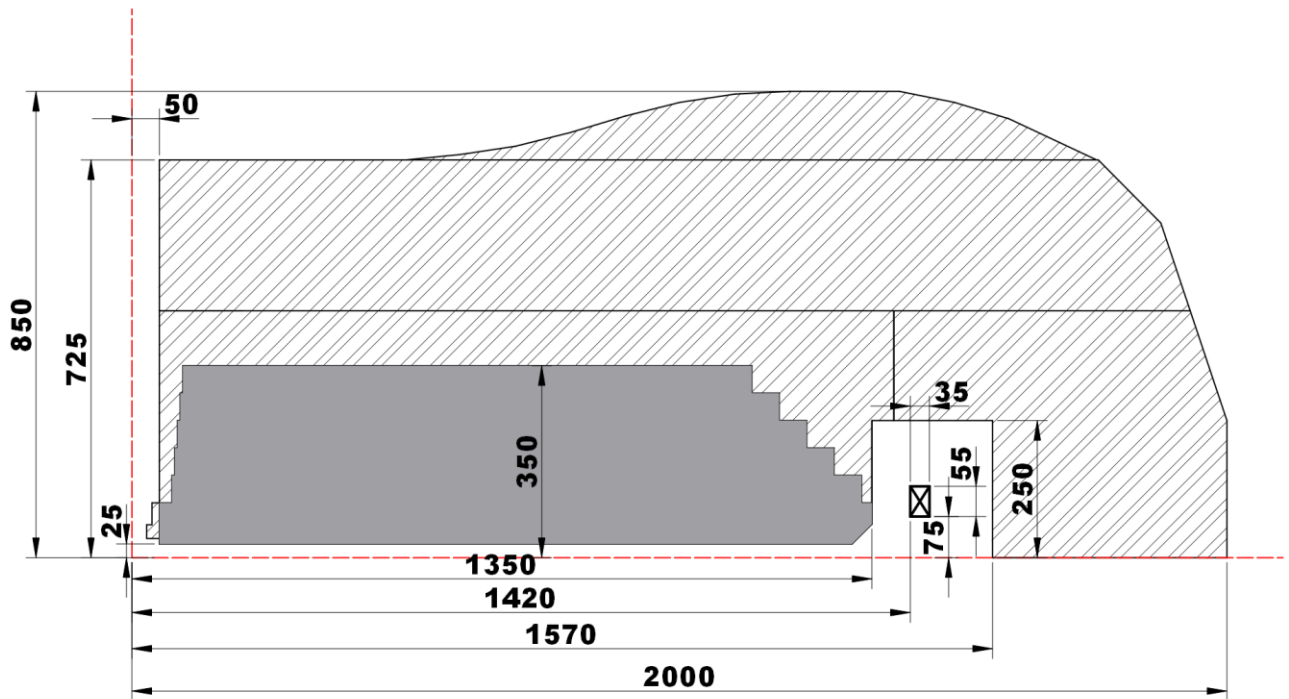


Figure 3: SC230 magnet yoke and SC coil general dimensions

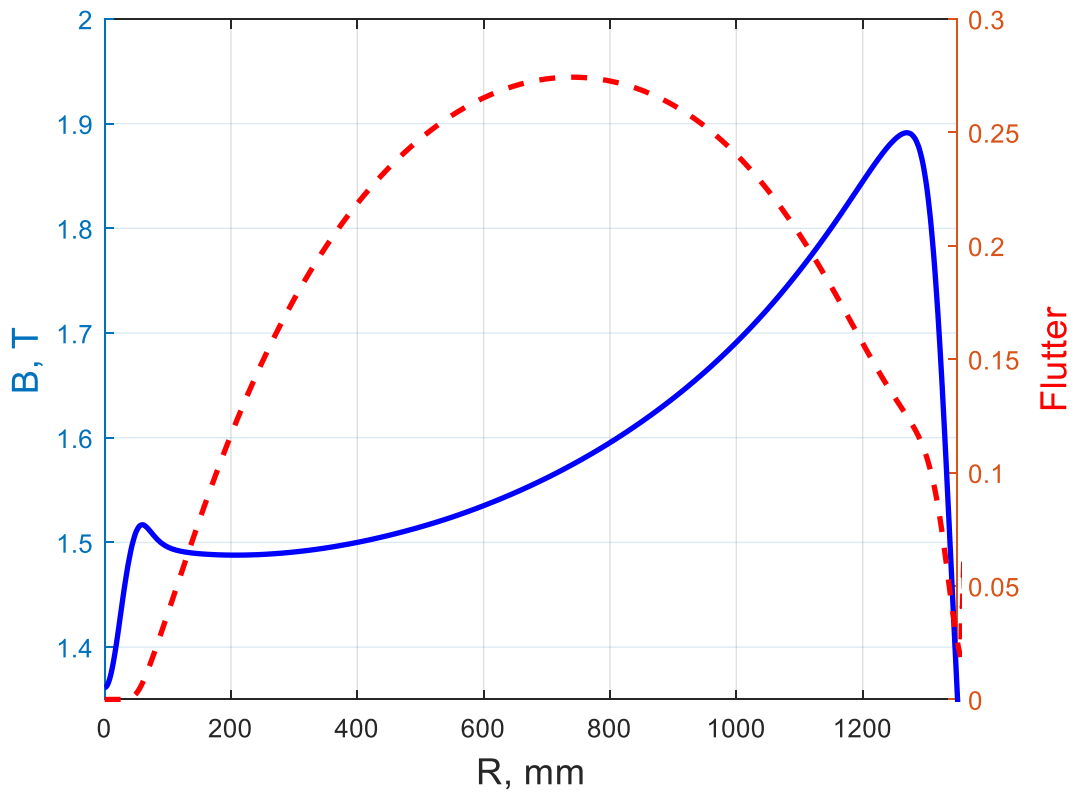


Figure 4: Average magnetic field and flutter along the radius.

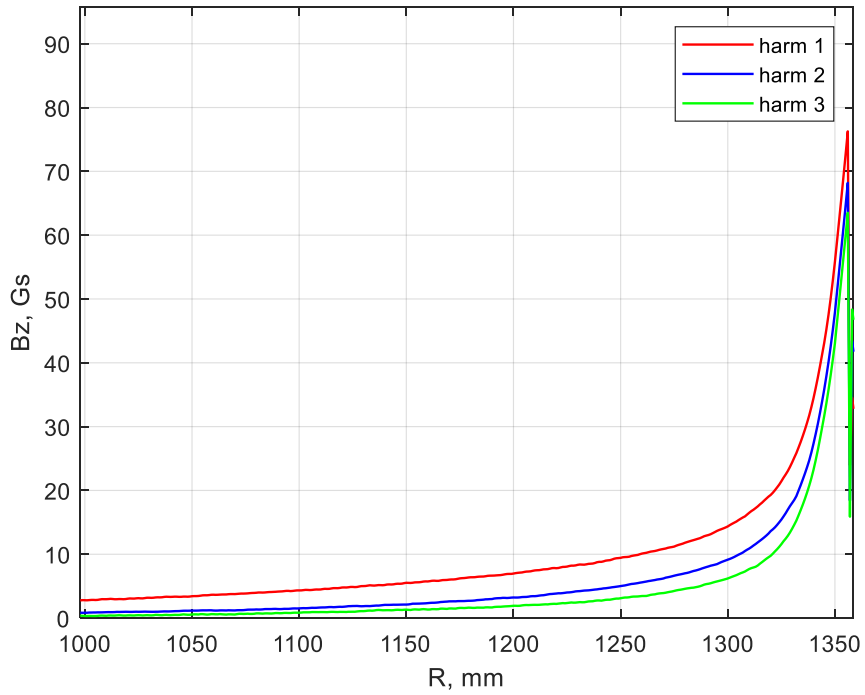


Figure 5: Low number harmonics

Magnetostatic forces exerted on SC230 magnet

The yoke and sector will be split on parts presented in Figure 6.

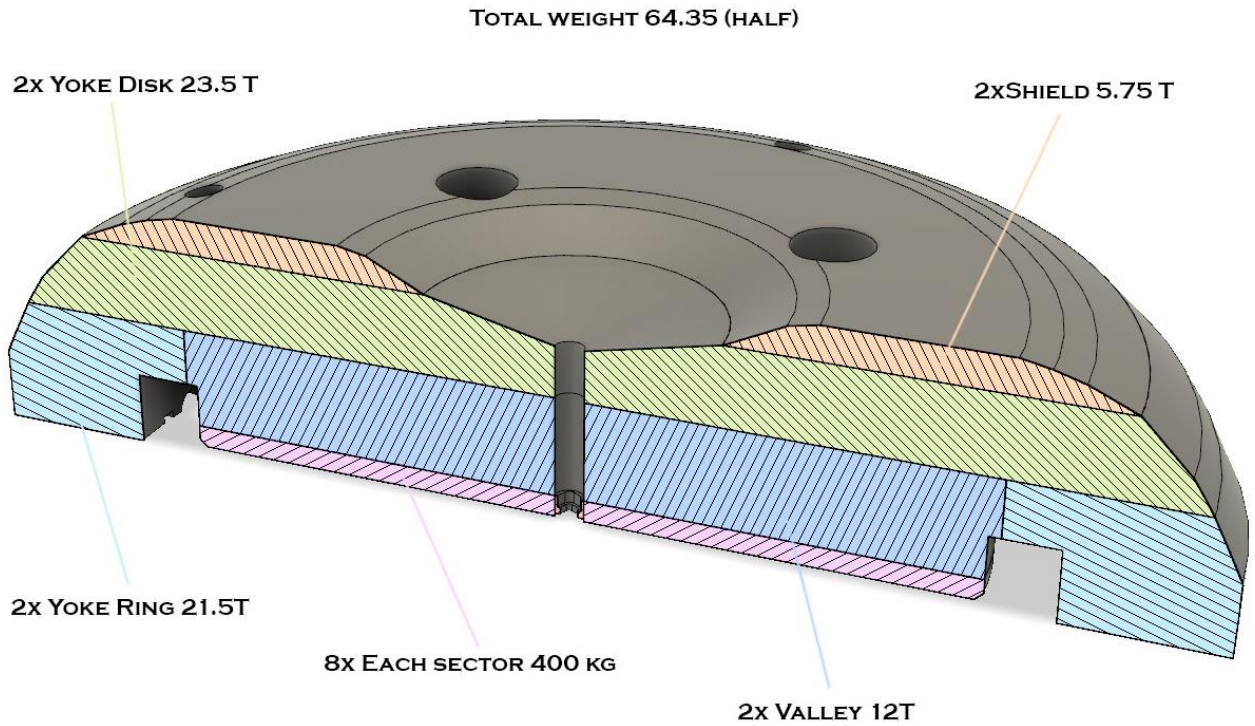


Figure 6: Weights of SC230 parts.

The calculation of the total magnetic force on an object in CST and Comsol performed through the closed surface integral of Maxwell Stress Tensor around that object. For the realistic force to be found object surrounded by a magnetic neutral material ($\mu = 1$), e.g. air.

- a) – gives you correct total force in calculation through any surface – A or B
- b) – gives you incorrect total force.

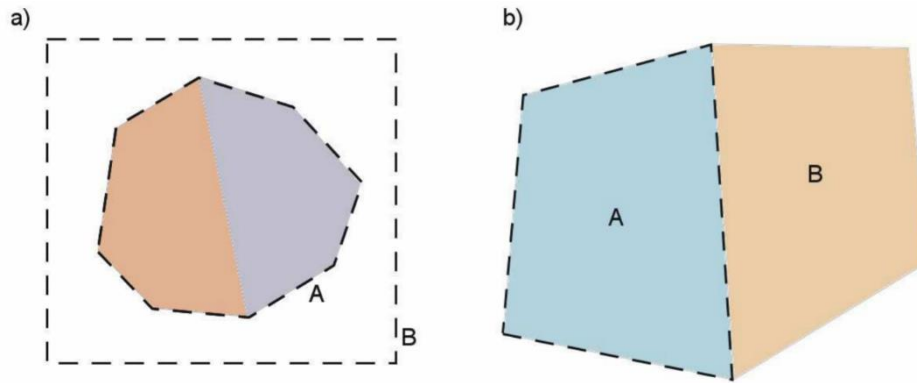


Figure 7:

$$\mathbf{F} = \frac{1}{\mu_0} \int \int dA \bar{\mathbf{S}} \cdot \mathbf{n}$$

$$\mathbf{S} = \frac{1}{\mu_0} \begin{bmatrix} B_x^2 - B^2/2 & B_x B_y & B_x B_z \\ B_y B_x & B_y^2 - B^2/2 & B_y B_z \\ B_z B_x & B_z B_y & B_z^2 - B^2/2 \end{bmatrix}$$

The parts of SC230 magnet were separated with thin 0.1 mm layers of air filled with robust mesh (up to 6M elements per model) for accurate force calculation.

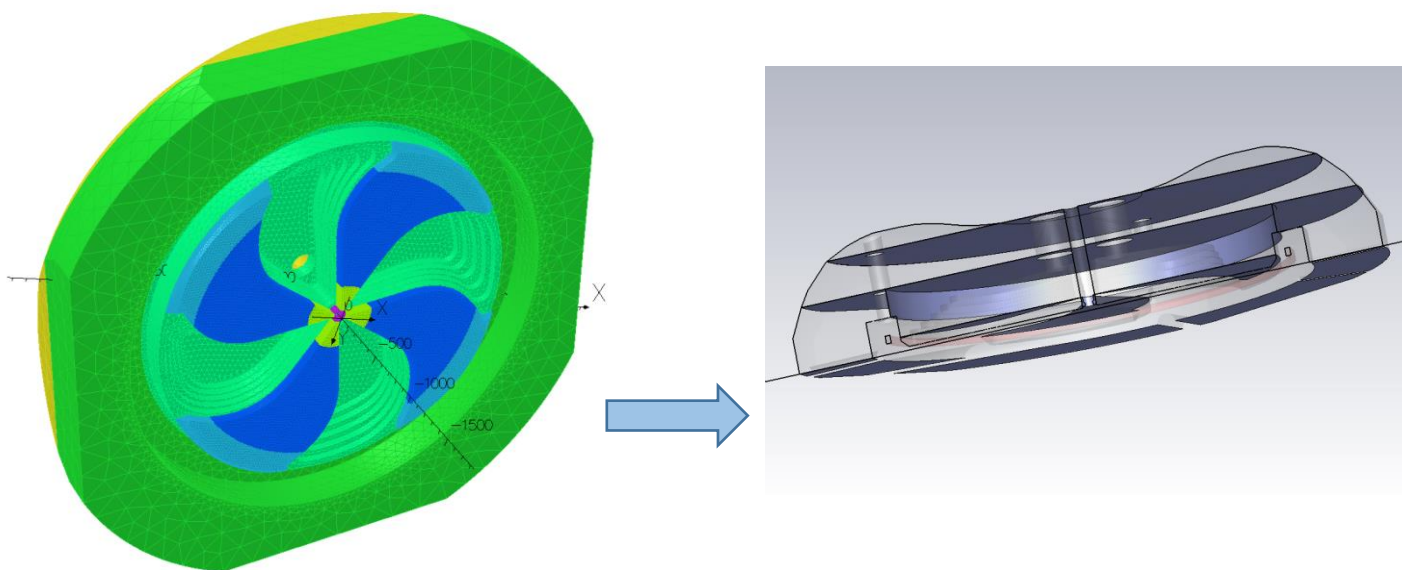
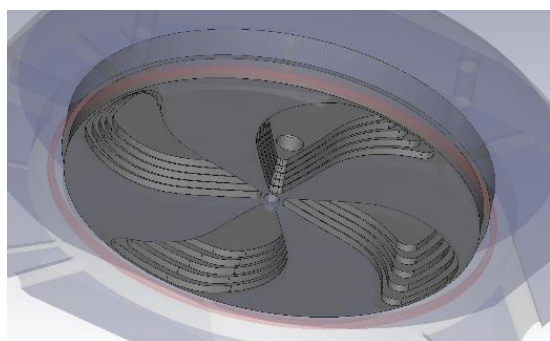
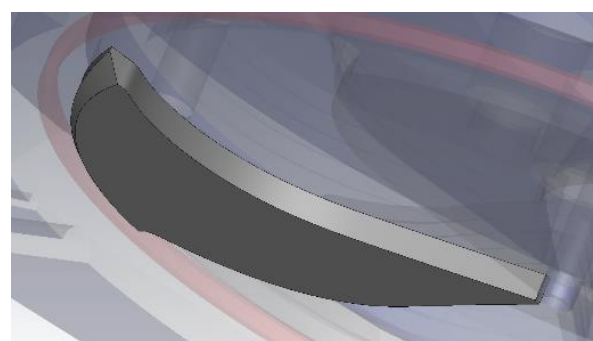


Figure 8: Model partitioning



Base



Sector

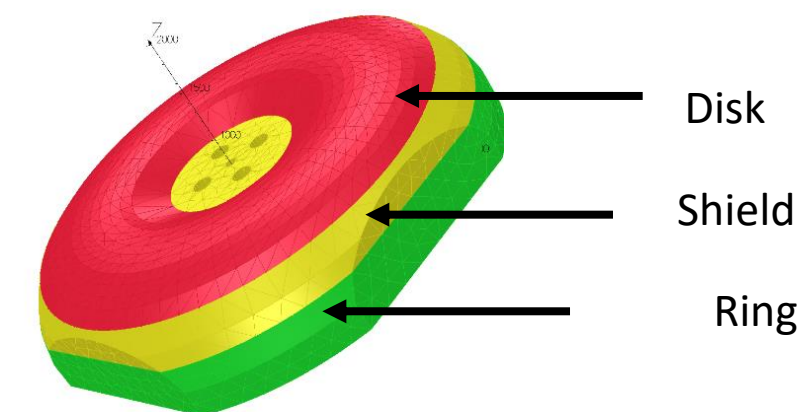


Figure 9: Parts of magnet

Forces were calculated in the variety of models and meshes. So the reliability of the results was checked in CST environment. You can see them in the Table 6.

CST results differ from TOSCA's because we used different magnet models.

Table 6.

Element	Force, CST (Popov) (tonnes)	Force, TOSCA (Ivanenko) (tonnes)
Sector	16	22
Base	-501	-390
Disk	-614	-700
Shield	-89	-160
Ring	-446	

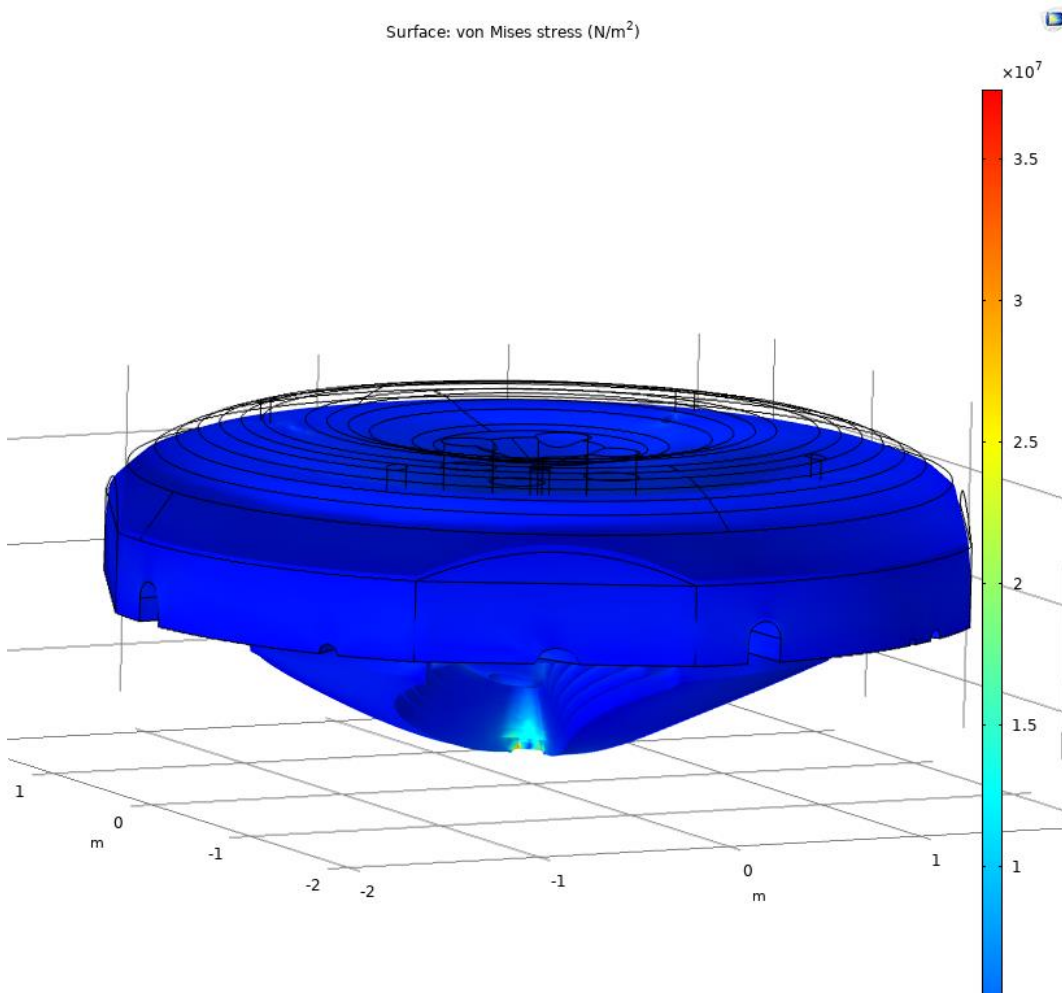


Figure 10: Stress simulation in COMSOL.

Deformation * 1e4

The iron elements forces leads to the maximum magnet deformation (in the center) ~ less than 0.1 mm.

Need more detailed study with exact screws locations and dimension => TBD during detailed engineering design.

Vertical Force between coils is about 1 tonnes (to the median plane) for S200 Fz = 100 tonnes

Table 7. Magnet parameters.

Yoke material	St.1010
Average magnetic field ($R_o/R_{extr.}$), T	1.5/1.9
Extraction radius, m	1.27
Pole diameter, m	2.7
Magnet diameter, m	4
Magnet height, m	1.64
Hill gap, m	0.05
Valley gap, max,m	0.7
A*turns, (1 coil)	170 000
Magnetic field in the coil, T (max.)	2.0
Cryostat and coils weight, tonne	5
Magnet weight, tonne	130
Coil dimensions,mm ²	55x35
Vertical gap between coils, mm	150

2. EQUILIBRIUM ORBIT CALCULATION

A number of beam dynamics simulations were performed during design of the magnet system.

They are:

1. Equilibrium orbit analysis to reach proper isochronism and focusing,
2. Beam dynamics simulation to check correctness of model and possibility of efficient extraction by tracking.

During the magnet simulations the following design goals were achieved:

- Isochronous field in the whole accelerating range;
- Last orbit of the circulating particle was kept close to pole edge of 10-15 mm;
- The stray fields were kept at an acceptable level;

- Dangerous resonances were avoided.

Isochronism of the average field was reached via a change of the sector's width. Azimuthal width of the sector changed along the radius from center to extraction from 25 to 40 degrees.

Orbital frequencies of the reference particles in the final average field are presented in Figure 11. From Figure 11 we can estimate that the difference between the mean field and the isochronous field is about 5 G in accelerating region. We would like to notice that all results look smoothed and were obtained with a rather low number of mesh cells (about 4 millions) in CST.

Betatron tunes calculated for a sample set of energies with CYCLOPS-like code are presented in Figure 12.

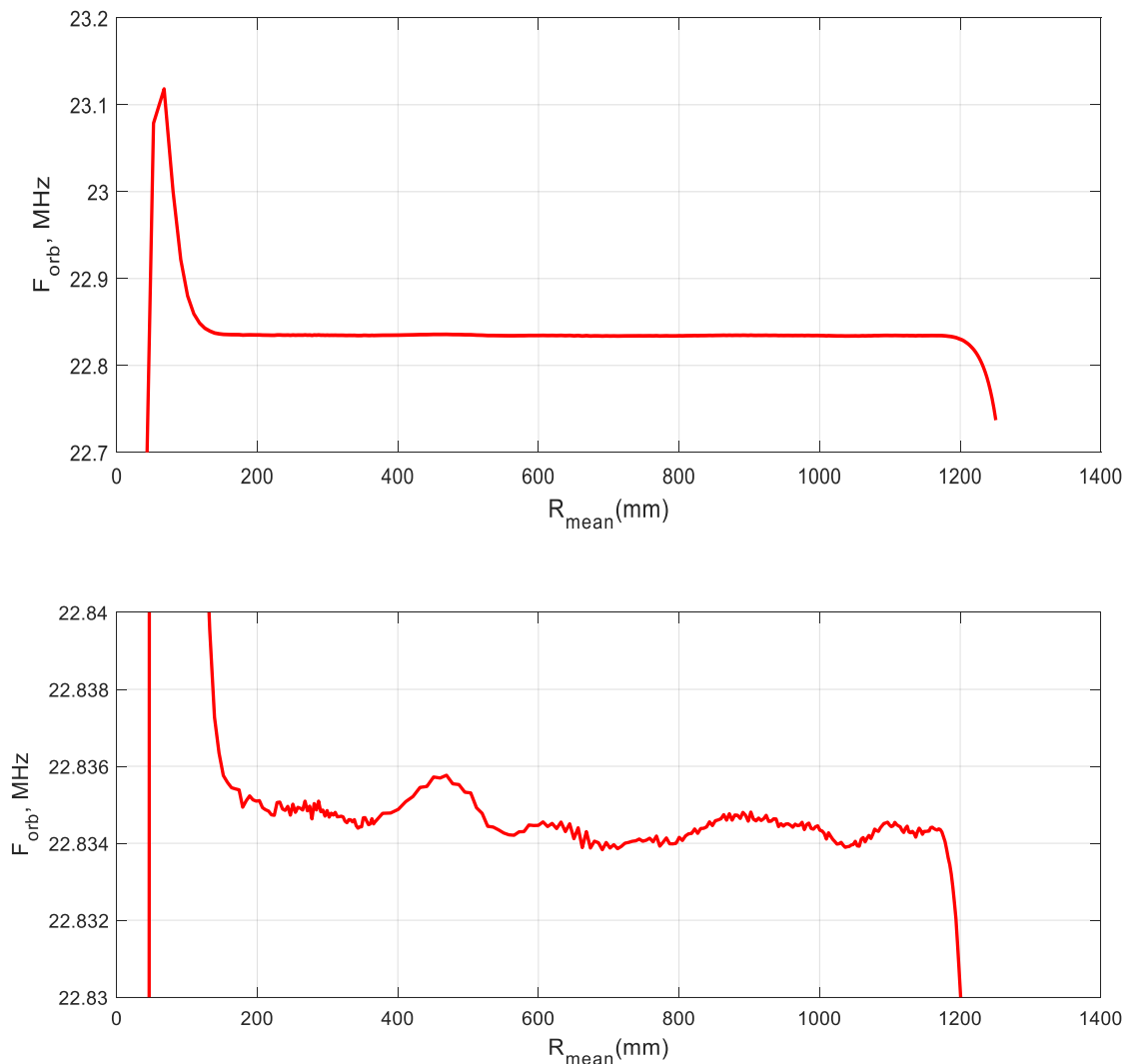


Figure 11: Orbital frequency against mean radius.

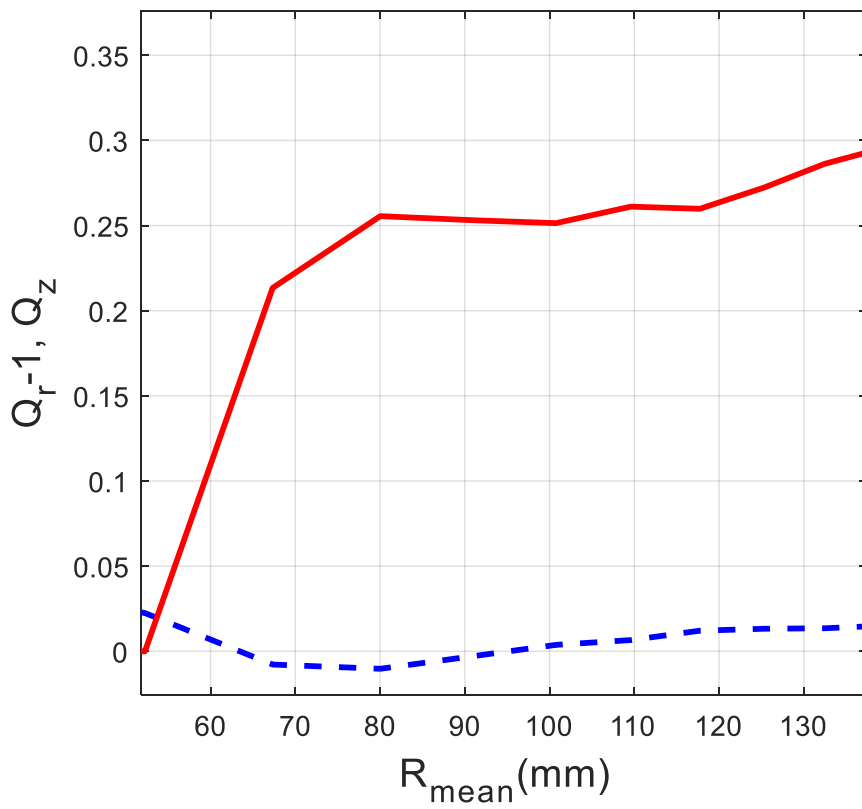
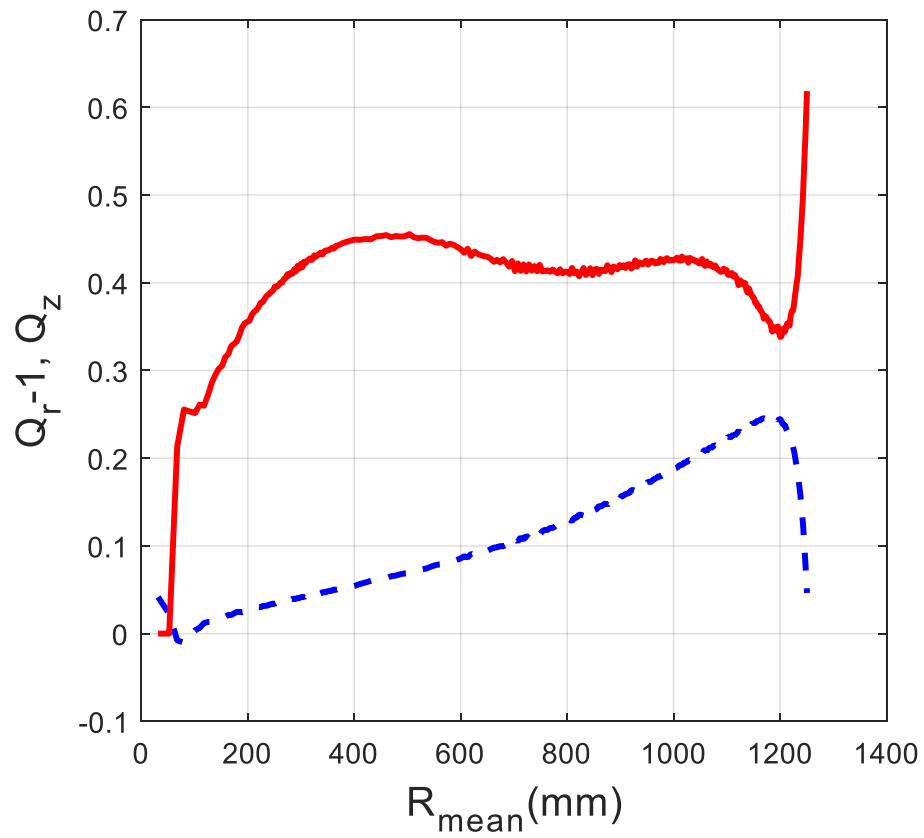


Figure 12: Vertical and radial betatron tunes in SC230.

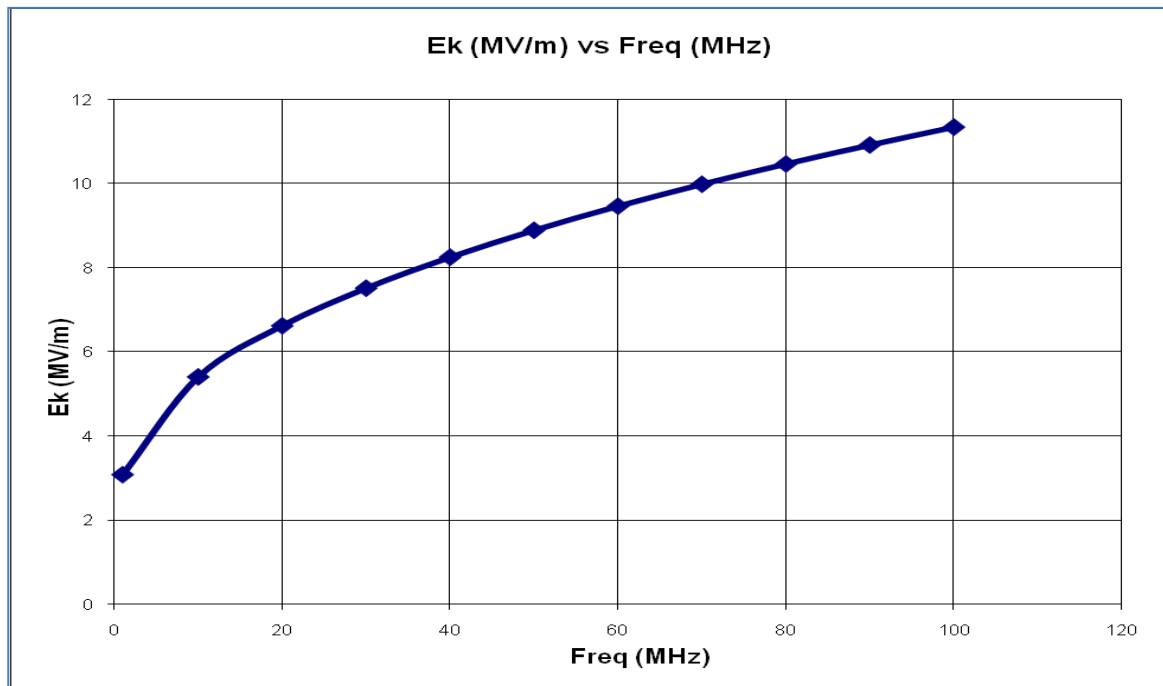
3. PRELIMINARY BEAM DYNAMICSESTIMATIONS

In order to have efficient center region we create a bump in the magnetic field. The bump value should be about 150-200 G.Magnetic focusing induced by the bump occurs after the radius R=50mm.For the radius less than 5 cm vertical focusing is provided for lagging particles by electric accelerating field.

Internal PIG proton source with hot cathode will be used in our cyclotron and will provide current at least 50 μA[9].We plan to use a rather small voltage of about 40-50kV in the center to avoid sparking.Accurate 3D model of the source and the central region is described in Ch.5.

The voltage should satisfy Killpatrick criteria for the sparking.

$$f = 1.643 * 10^{-2} E_s^2 * e^{\frac{-85}{E_s}}$$



4.

Figure 13: Killpatrick criteria

For $f_{rf}=91$ MHz Killpatrick limit is about 11 MV/m. Vertically we will have field: $50kV/25mm=2$ MV/m much less Killpatrick limit.

Isochronism of the model is good enough and can be corrected at the last stage after we finally fix the design of the cryostat and of the superconducting coils.The beam has been accelerated in the 3D magnetic and 3D RF electric field maps with amplitudes of betatron oscillations up to $A_r=2$ mmz=3mm. There were no losses of particles at any radius after center region. No influence of any resonance was observed. We succeed in acceleration up to the edge of the sectors of the cyclotron

which are cut along the trajectory and have a chamfer which helps with providing necessary increase of the field.

Acceleration takes about 600 turns beginning from energy 100 keV to 233MeV. Voltage = 1.1*voltage from Figure 23.

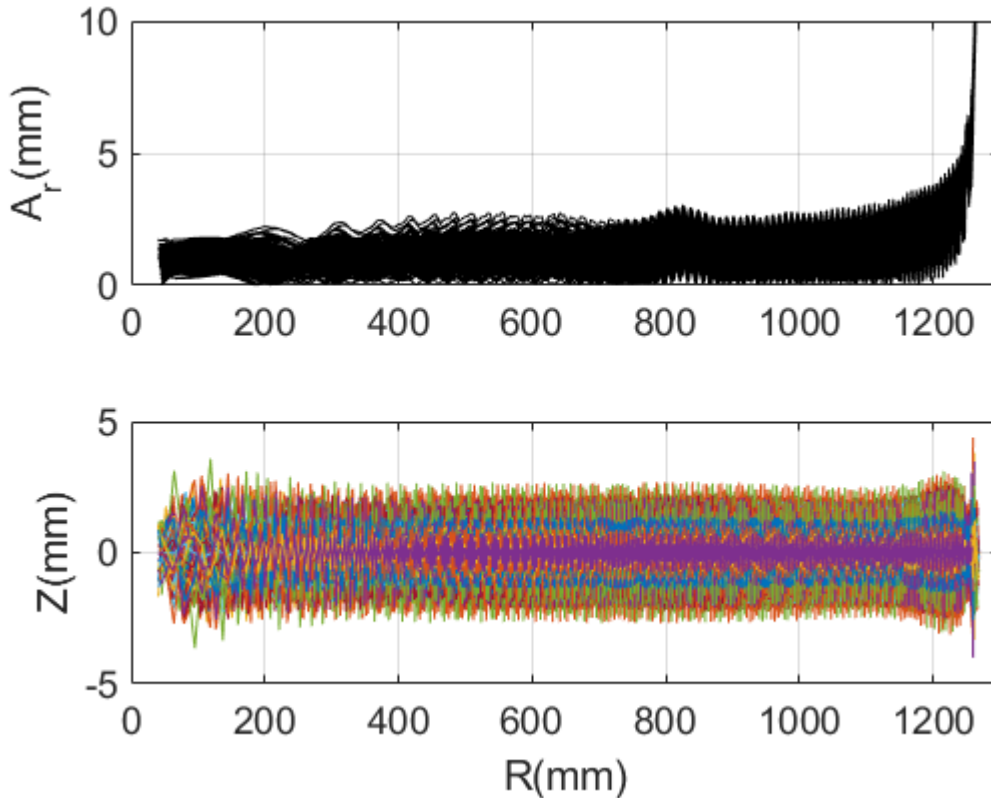


Figure 14: Amplitudes of radial oscillations and vertical motion of the beam.

Preliminary simulations show that the extraction can be carried out by two deflectors with less than 100 kV/cm electric field placed between sectors. Tracking performed without magnetic channel (MC), suitable azimuthal position for MC is marked (see Figure 15). MC1 should be placed close to the sector on azimuth 180° to conserve beam quality and achieve horizontal focusing. Focusing of the beam in the vertical plane is provided by a drop of edge magnetic field. The collimator and quadrupoles can be used to match the beam parameters with requirements imposed by a transport system after exit from cyclotron.

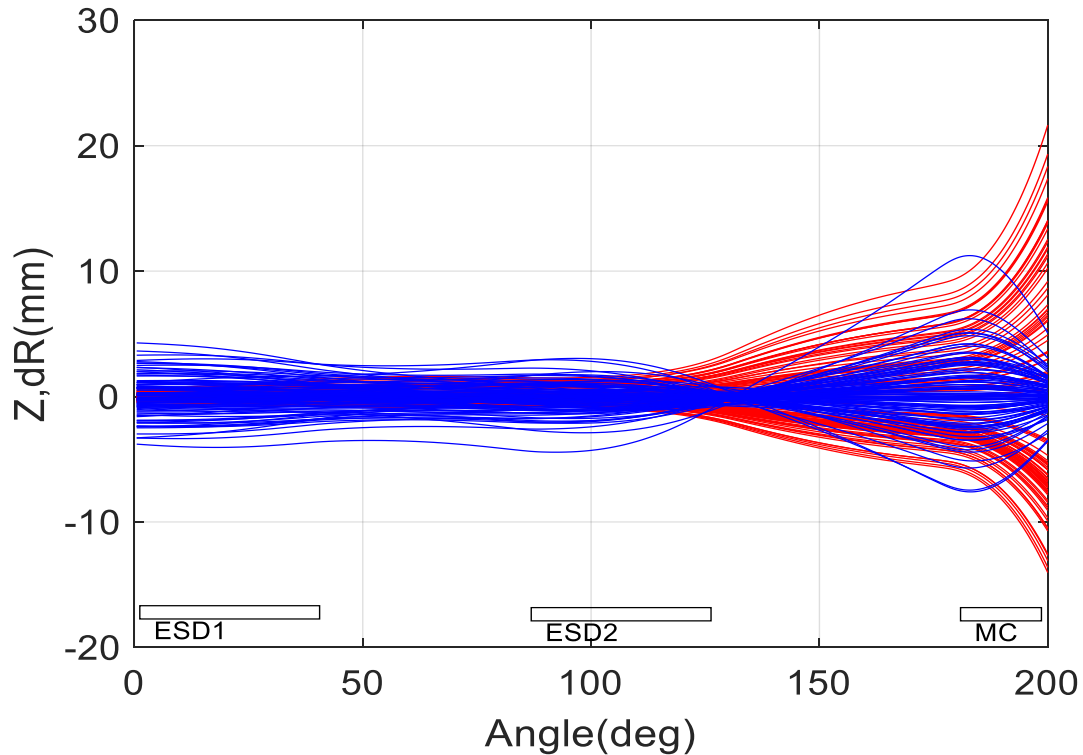


Figure 15: Beam path through the ES deflectors, red lines-horizantal, blue lines – vertical motion.

Suitable positions for gradient correctoris marked by MC.

This proposal has 2 Chapters devoted to beam dynamics in SC230. Beam dynamics simulations in this chapter were performed without any simplifications but began from energy 100 keV (after two accelerating gaps) in non optimal center (see Figure 16).

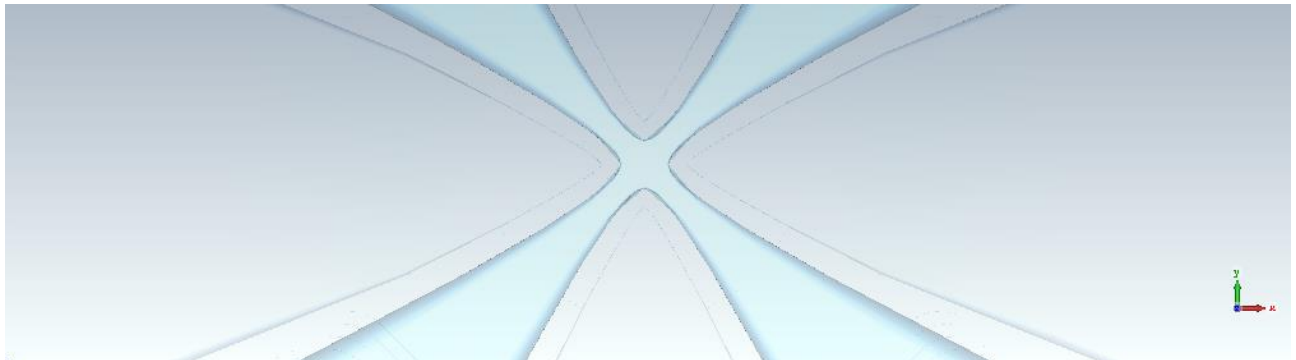


Figure 16 View of the center region used in simulations Ch.3.

Carefully designed center region and extraction schema is presented and analyzed in the Ch.6. Simulations in the accelerating region in Ch.3 and Ch.6 were performed by different codes based on equations of motion with different independent variable (azimuth angle in Matlab code, time - in SNOP code [10]) has different approach in accelerating field presentation. The only difference observed in results received by both codes is in the number of turns in accelerator. The reason is in difference in accelerating voltage. Ch 6 describes dynamic with linear voltage along the radius and

Ch.3 field map from RF simulation was used (voltage along radius can be seen in Figure 23). So more accurate estimation of number of turns is from Ch.3 and it is about 600. In both simulations there were any resonance effects observed.

5. ACCELERATING SYSTEM DESIGN

RF cavities are located at the valleys of the magnet, the geometry of the RF cavity is restricted by the size of spiral sectors. For proton acceleration, we are planning to use 4 accelerating RF cavities, operating on the 4th harmonic mode. The choice of 4th harmonic is a natural choice for a cyclotron with 4 sector and provides high acceleration rate. All four RF cavities will be connected in the center and will be working on approximately 91.5 MHz frequency. Cavities can be equipped with an inductive coupling loop and will be adjusted by capacitance trimmers like in SC200[8].

Computer model

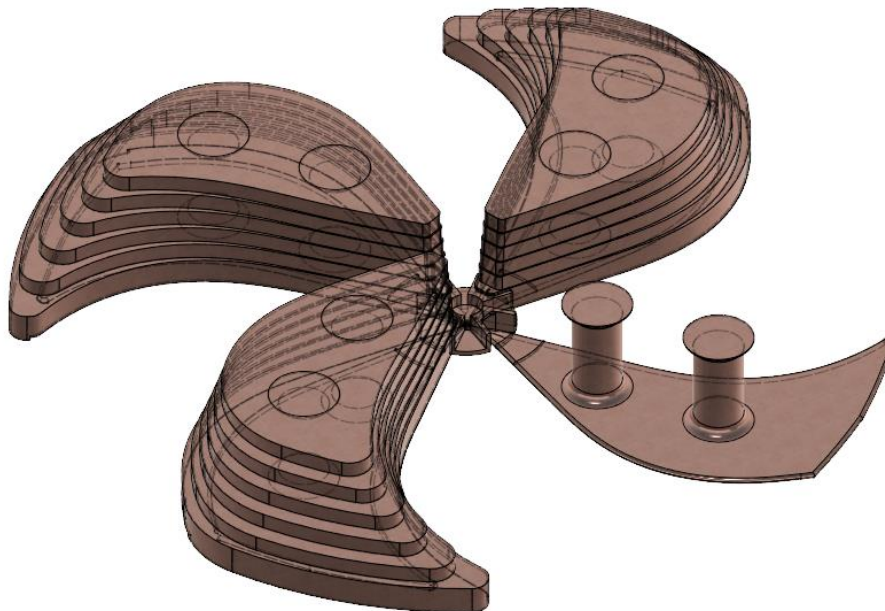


Figure 17: Overview of 3D model of RF system.

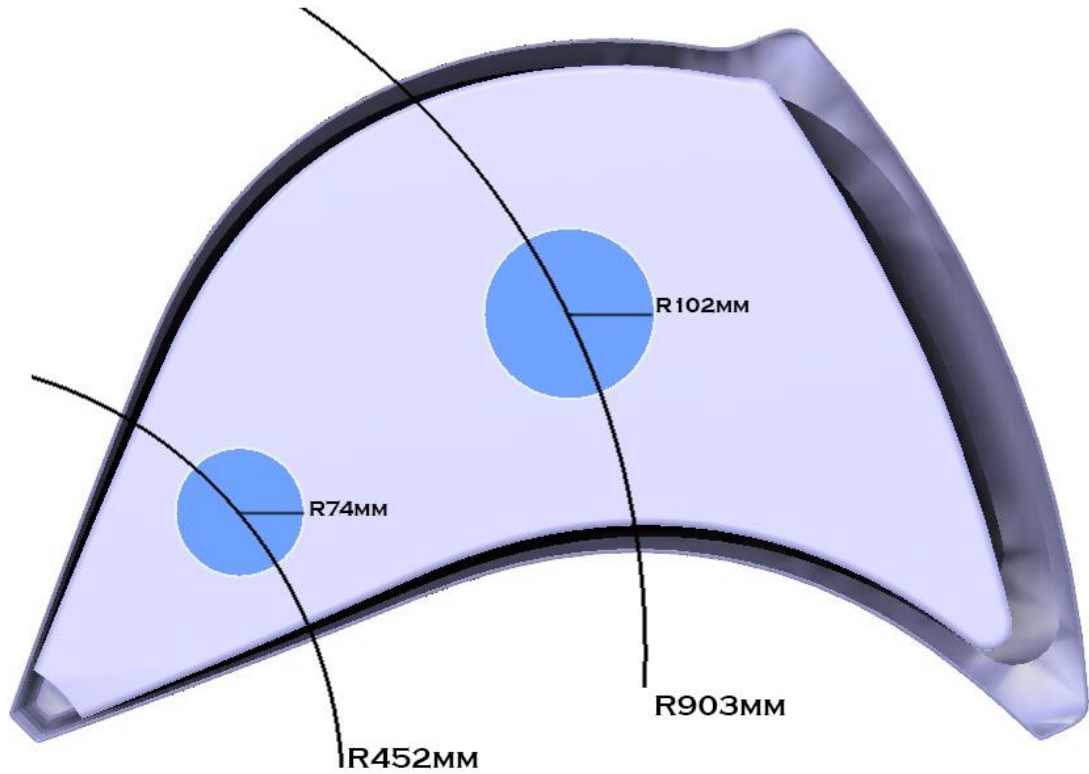


Figure 18: Accelerating cavity.

The characteristic parameters of the half-wavelength coaxial resonant cavity with two stems have been obtained from simulation in CST studio. The RF cavity resonator solution for the SC230 cyclotron can be seen in Figure 17. Azimuthal extension of the cavity against radius is presented in Figure 19. Suitable accelerating frequency and voltage along radius were achieved. The calculation results of acceleration voltage are presented in Figure 23.

Table 8. Accelerating system parameters.

Frequency, MHz	91.5
Harmonic number	4
Number of cavities	4
Power losses, kW (total)	43
Q-factor	13800
Voltage center/extraction, kV	35/95

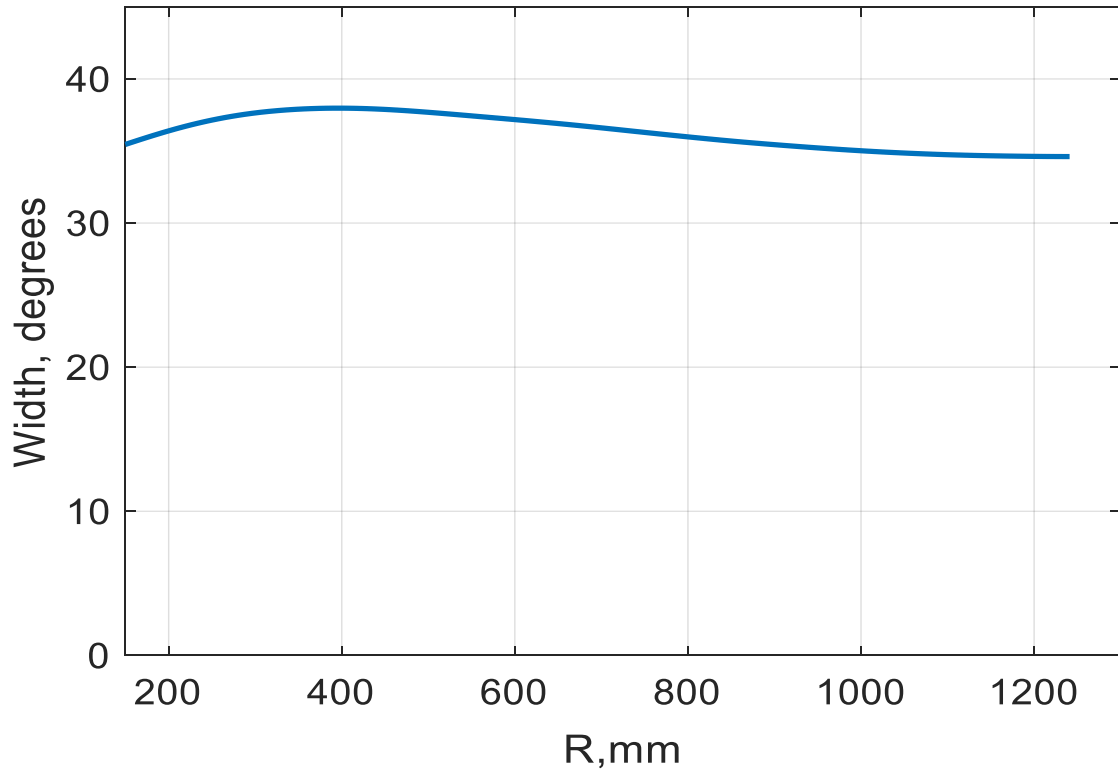


Figure 19: Azimuthal extension of the cavity (between middles of accelerating gaps).

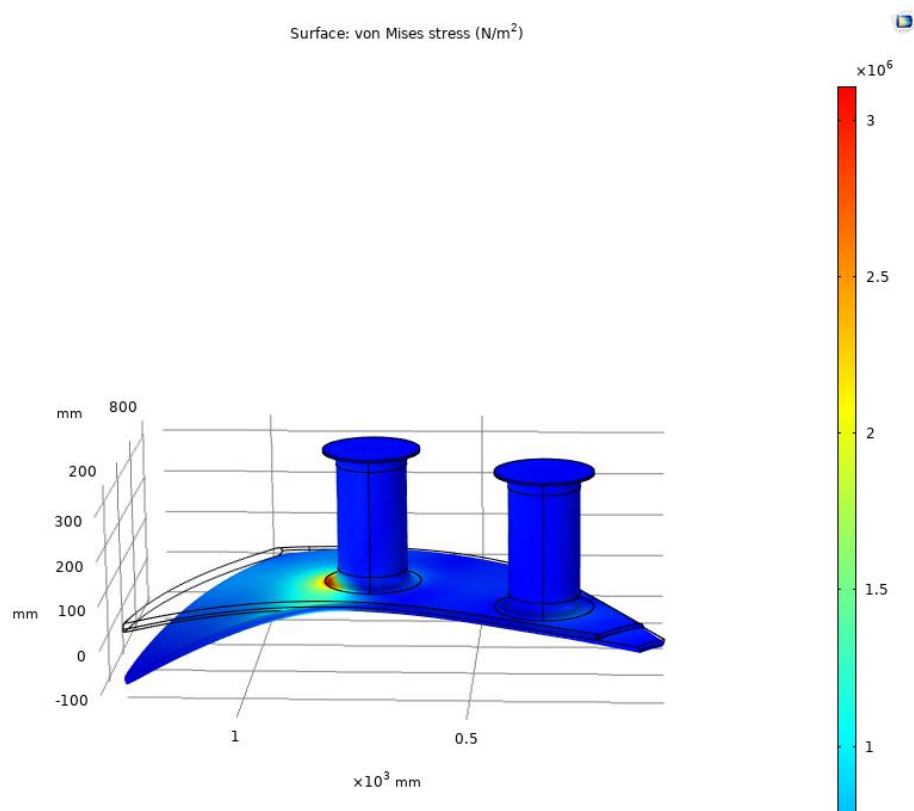


Figure 20 Stress analysis of the Dee

Design with 2 stems is good for mechanical rigidity (simulation from COMSOL Multiphysics).

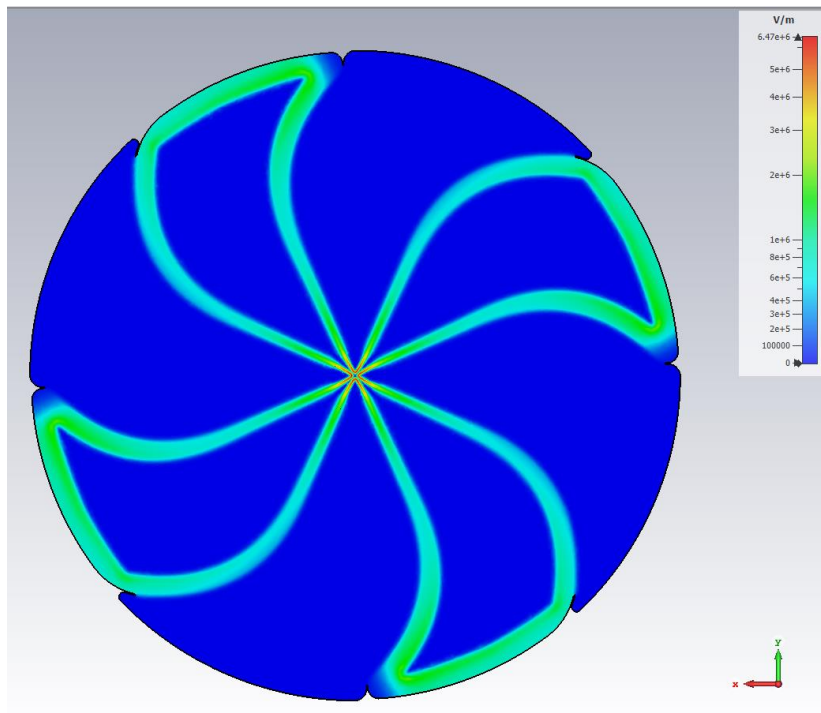


Figure 21: Electric field distribution

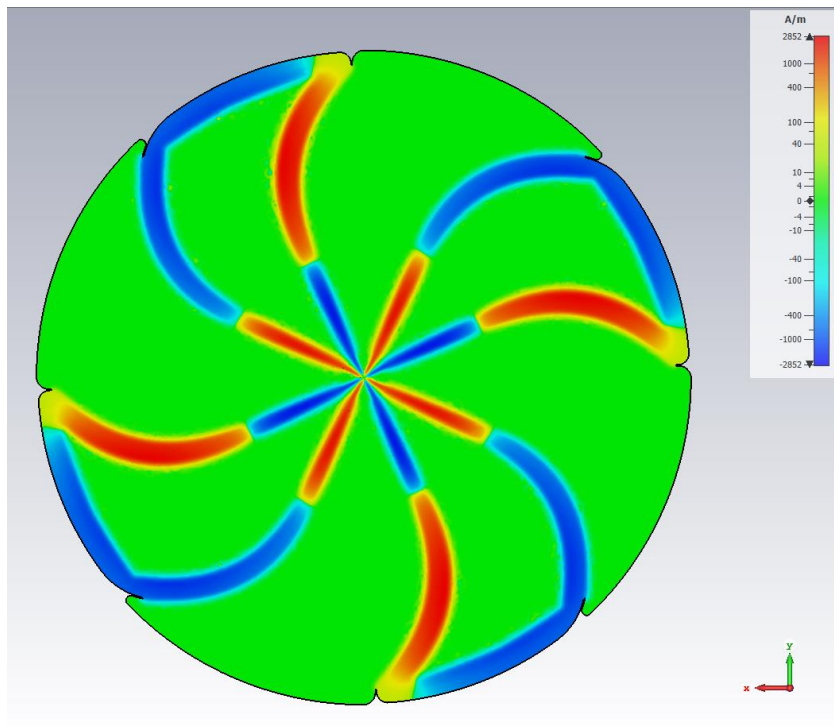


Figure 22 Magnetic field distribution

As the beam will be accelerated in the fourth harmonic mode we believe that the RF magnetic field will not have noticeable effect on the beam.

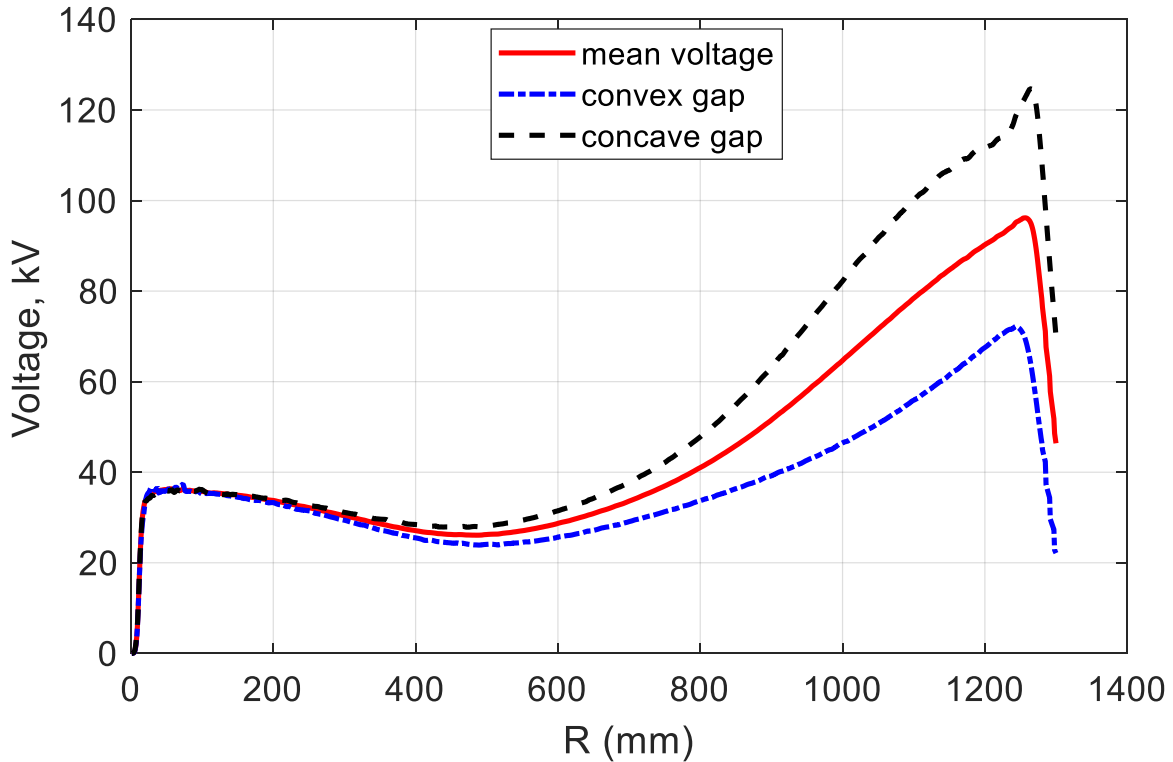


Figure 23: Accelerating voltage along radius.

The value of the accelerating voltage was obtained by integrating the electric field in the median plane of the resonant cavity along the arc of a circle for each gap separately.

Power losses.

Power dissipation in the model was calculated assuming the wall material is copper with a conductivity $\sigma = 5.8 \cdot 10^7 \text{ 1}/(\Omega\text{m})$. The quality factor was about 13800 and power losses of all cavities were:

- for storage energy 1 joule voltage in the center/extraction 35-95 kV, thermal losses are 43 kW,
- Overall power and cooling requirements of the RF system are rather small.

6. BEAM DYNAMICS ANALYSIS IN SC230 CYCLOTRON

Magnetic system of the SC230 cyclotron was designed before starting of the present study. Magnetic field was shaped carefully. Deviation of average field from isochronous curve in main acceleration region is not more than $\pm 5 \text{ Gs}$ (Figure 24)

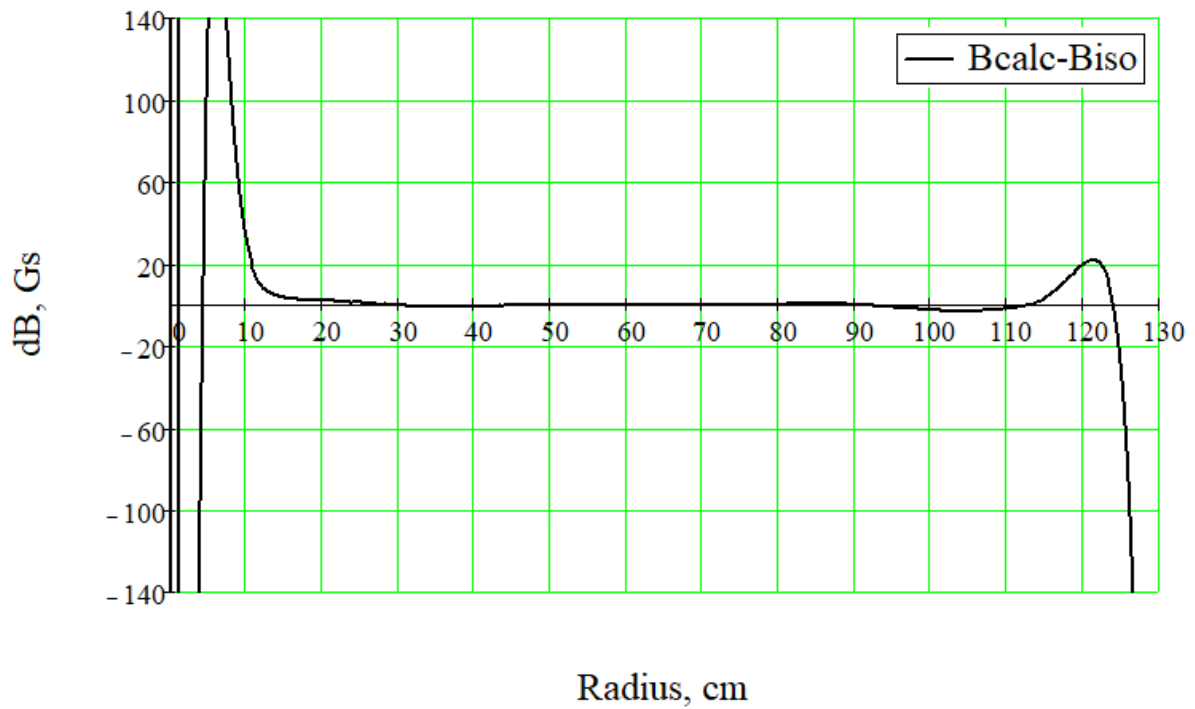


Figure 24. Difference between average magnetic field and isochronous curve. Accelerating frequency is 91.45 MHz.

Central plug was optimized in order to provide sufficient axial focusing of the beam in the central region. Value of field bump in the center is ~ 150 Gs providing shifting of average RF phase of the beam after central region to optimal energy gain (Figure 25).

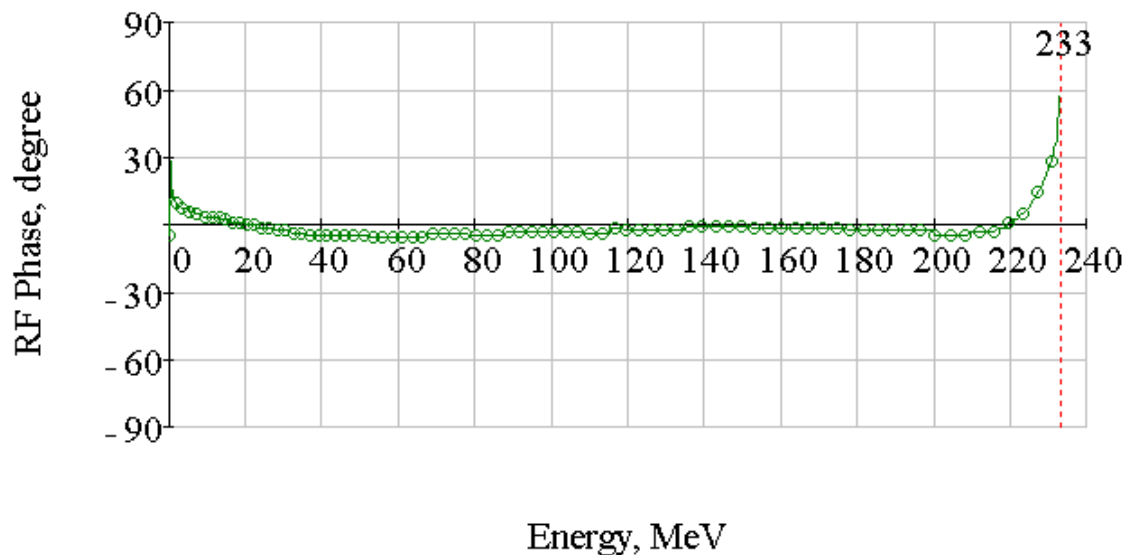


Figure 25. RF phase slip of a reference ion.

Axial hole in the plug has square shape (Figure 26) that is more suitable with internal ion source and allows minimizing of zone without axial focusing by magnetic field. The ion source is shifted from the cyclotron center by 15.8 mm. Particle tracing was performed with using 3D electrical field of dees. Peak dee voltage is increased from 50 kV in the center to 100 kV near the final radius. Number of turns of a reference ion is ~ 400 .

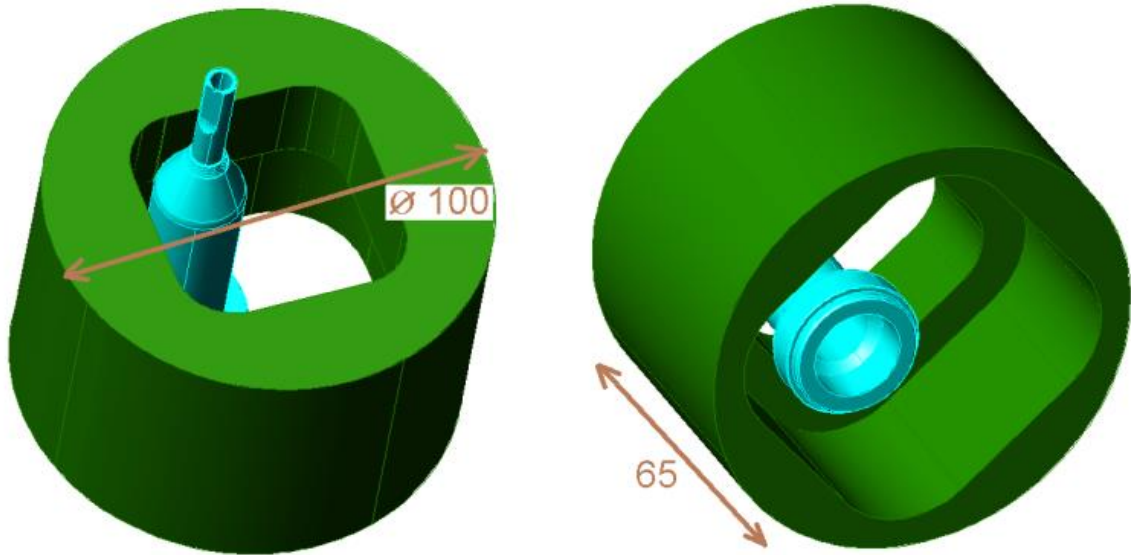


Figure 26. Location of the ion source in the central plug. Dimensions of the plug: diameter 100 mm, height 65 mm, distance from median plane 35 mm.

Analysis of betatron tunes shows that axial frequency Q_z is enough at all radii. This fact allows preventing of crossing of $Q_r - Q_z = 1$ resonance (Figure 27). Near the final radius crossing of $2Q_z = 1$ and $Q_r - 2Q_z = 0$ resonances takes place. At the final orbit radial frequency Q_r is near unity. Calculations of beam dynamics show that with enough radial quality of the beam near the final radius negative effects of mentioned resonances on the beam are missing.

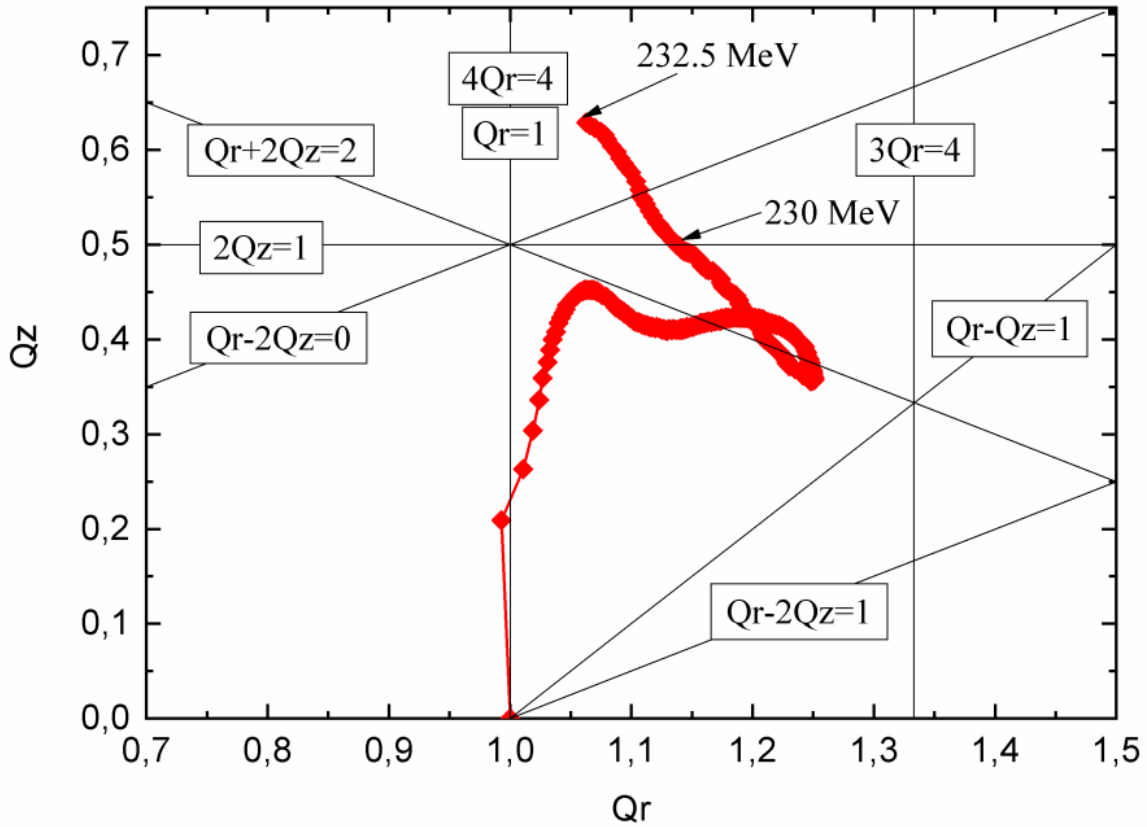


Figure 27. Tune diagram calculated by tracing.

The main goal of this work is a design of the cyclotron central region and extraction system. Requirements for extracted beam are: current is more than 500 nA; transversal geometrical emittances are about $5 \pi \cdot \text{mm} \cdot \text{mrad}$; energy spread is less than $\pm 0.2\%$.

For calculations of 3D electrical and magnetic fields Tosca/Opera3D was used. Beam dynamics analysis was performed with using SNOP code [10]. The study was based on using 3D fields of the structure elements. Realistic analysis of the beam losses on the structure surfaces was taken into account.

Central region

The sensitive central region design, which affects the entire acceleration characteristics for a given magnetic and electrical fields, is very difficult task to perform. A high axial beam quality and centering should be provided in search of a central region configuration at first turn. Also, the central region structure should be optimized for selection of the required RF phase range of the accelerated beam. The technical realization of the cyclotron ion source should be the same with the construction used in the SC200 cyclotron [11], which has been experimentally tested and

demonstrated necessary parameters of exiting beam. Having in mind corresponding measurements on the cyclotron, it can be predicted that the beam exiting the ion source will be in excess of 28-30 μA (peak current of 100 μA). The ion source slit has rectangular form with dimensions $0.5 \times 2 \text{ mm}^2$. On initial turns the size of the accelerating gaps is larger than 3.6 mm, which prevents sparking initialization at the peak dee voltage of 50 kV. Axial aperture of the dees increases from 5 mm at first turns to 20 mm in main accelerating zone. Axial distance between the dees and the central plug is 27 mm. The central region structure is shown in Figure 28.

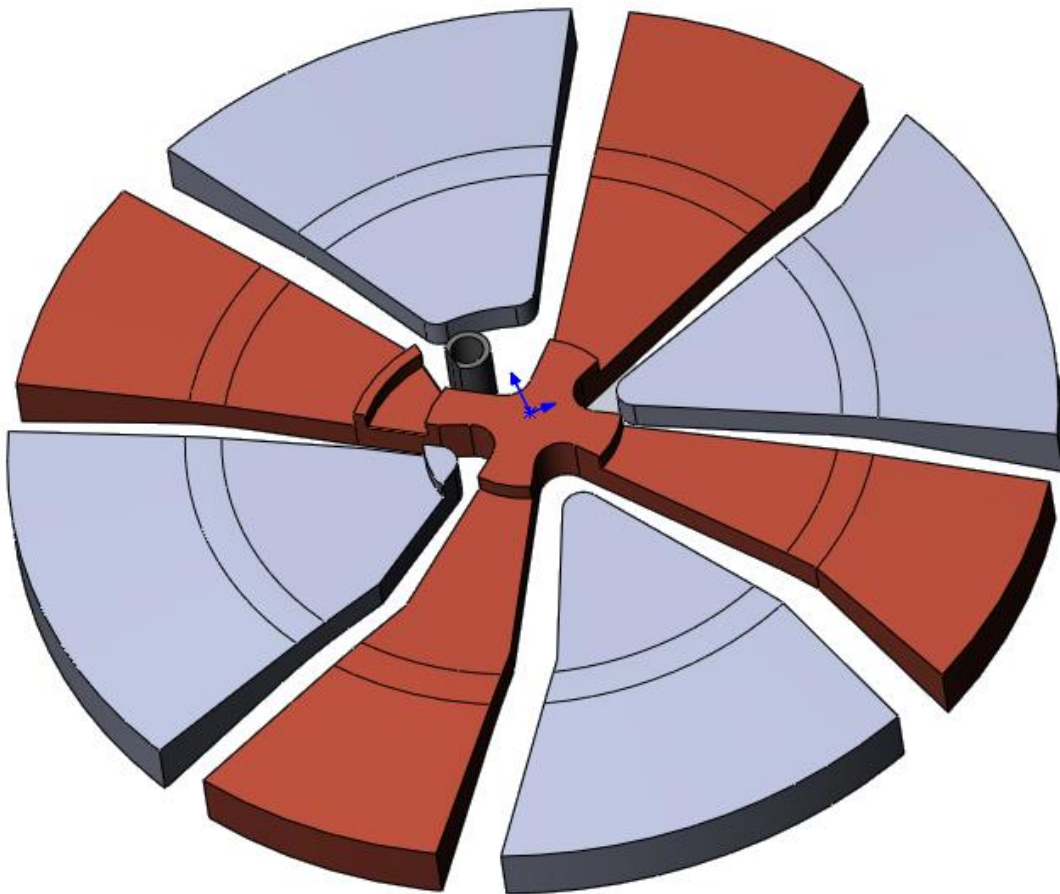


Figure 28. Central region structure.

Since axial focusing by magnetic field begins only from radius of 6 cm, it is necessary to design the central region under criterion having axial focusing by electrical field of the dees there. As a result, the developed structure provides passing of the first accelerating gaps by the beam with the accelerating field is decreasing. It means in case of using the *cos*-likefunction for specification of the accelerating wave, the RF phase is positive when an ion crosses a gap (Figure 29).

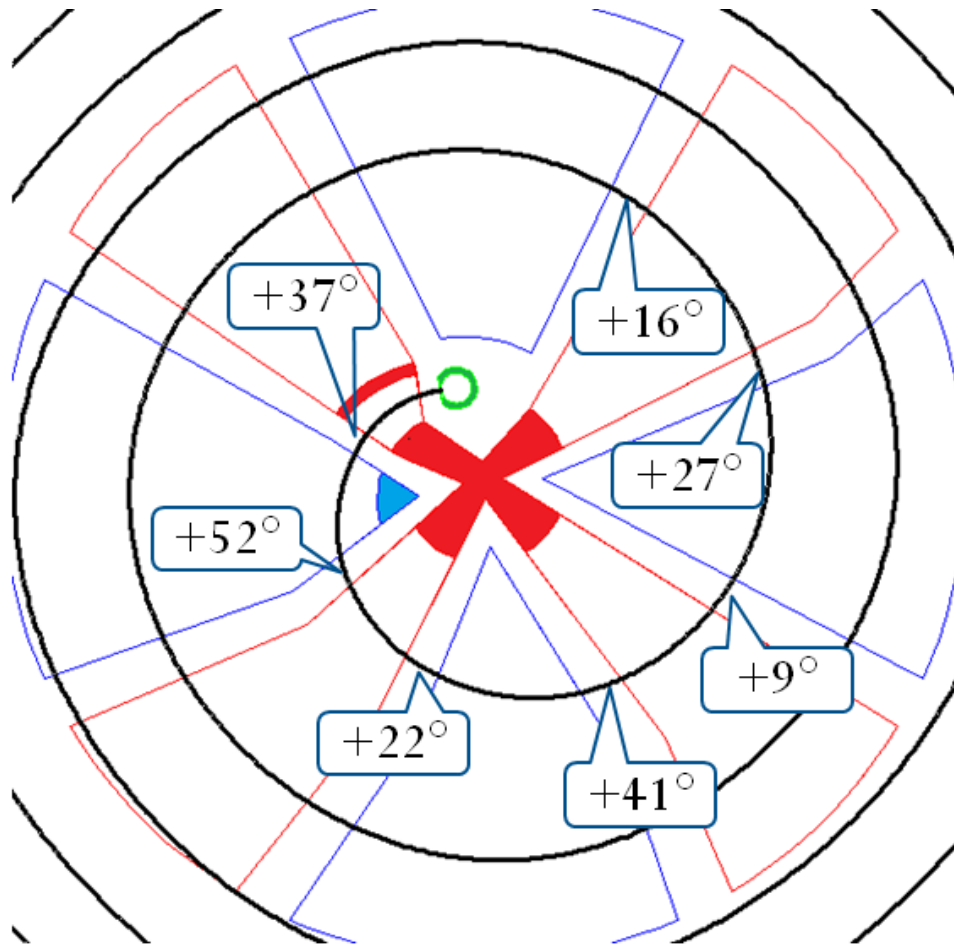


Figure 29. Trajectory of a reference ion in the central region. RF phase when particle crosses accelerating gaps is shown.

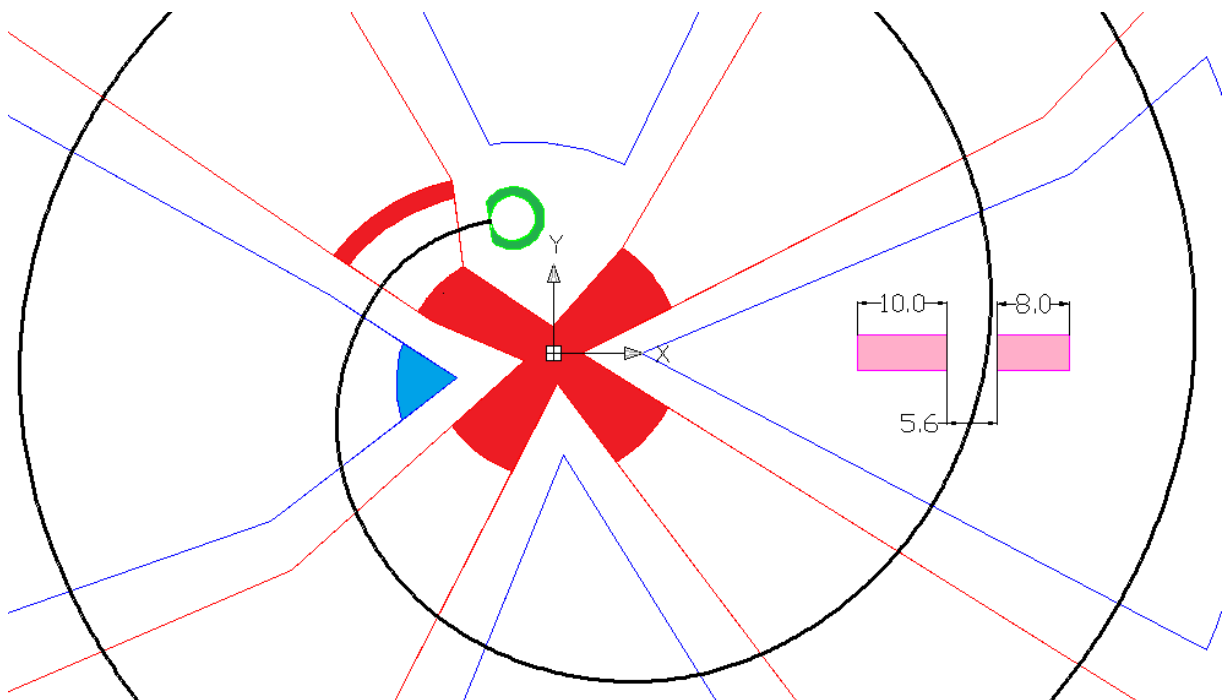
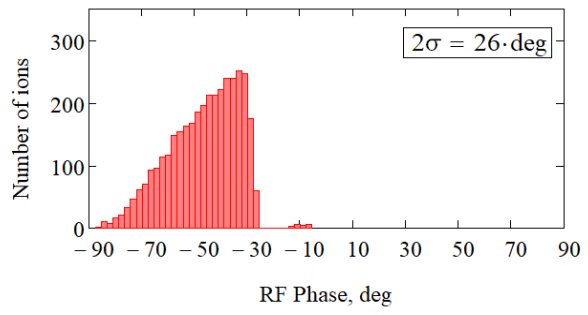
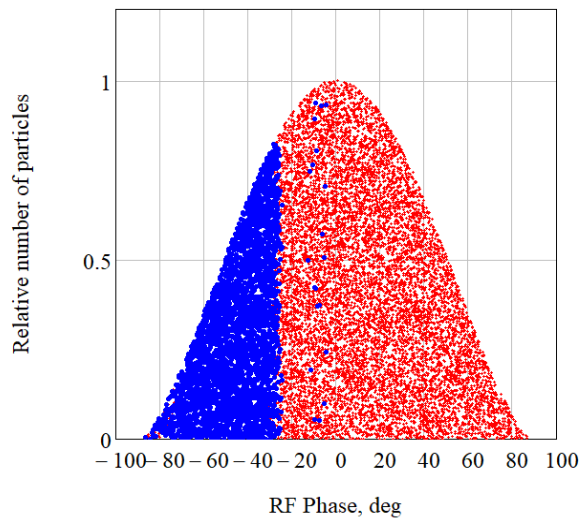
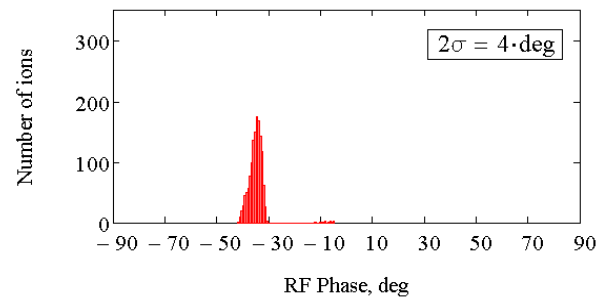
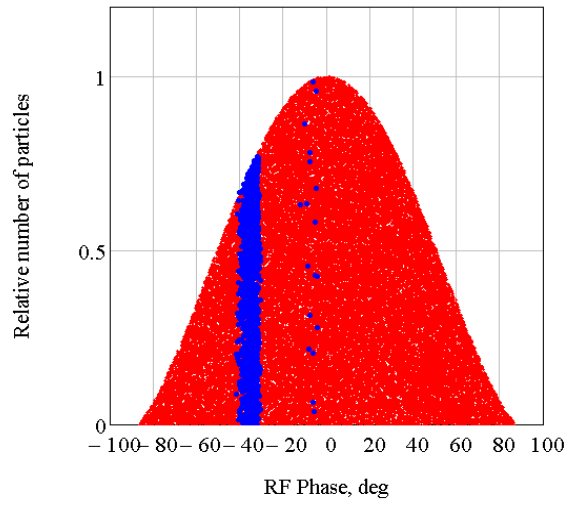


Figure 30. Location of the phase slit in the central region (12-deg bunch regime).



a)



b)

Figure 31. RF phase acceptance of the central region. Red points are ions in the initial injected beam at the IS slit, blue dots are particles accepted into acceleration. Structure without phase slit (Beam transmission through the central region is 25%. Average RF phase is -45 degree) – (a). Structure with phase slit (8-deg bunch regime. Beam transmission through the central region is 2.6%. Average RF phase is -35 degree) – (b).

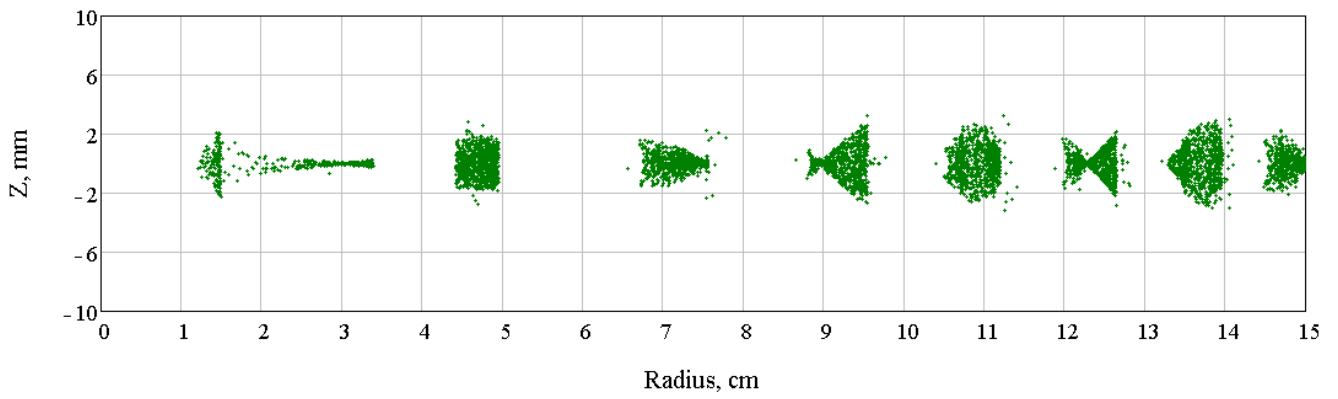


Figure 32. Axial motion of the beam in the central region (structure with phase slit).

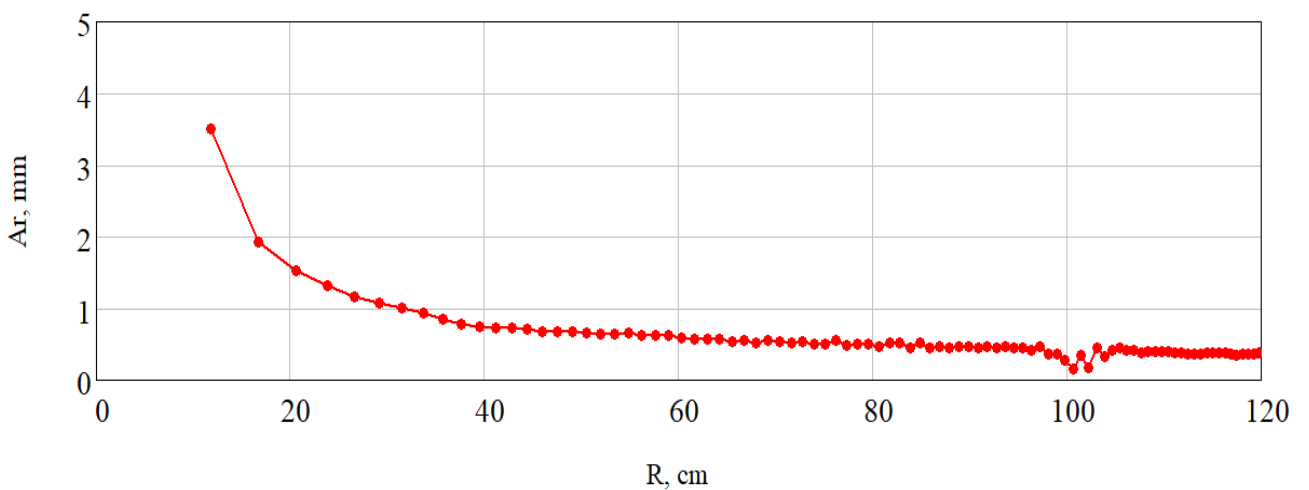
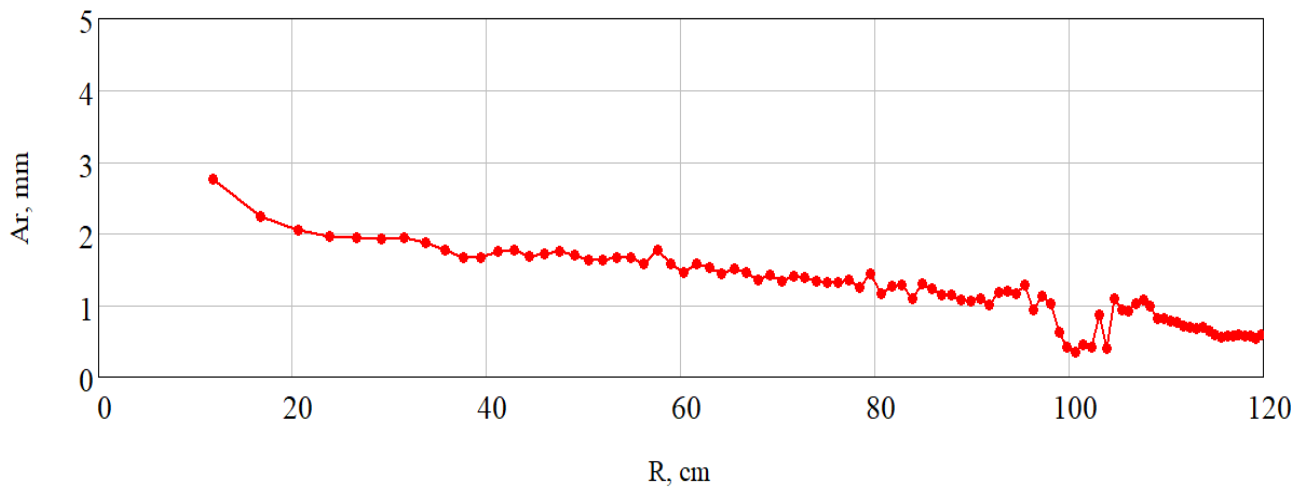


Figure 33. Amplitudes of radial betatron oscillations of the reference ion without 1st harmonic in the central region (upper plot) and with 1st harmonic of 10 Gs at radius 10 cm (lower).

The medical application of the cyclotron dictates special requirements to the parameters of the output beam from the machine. The final energy of the beam and related to it radiation losses during the extraction process impose related limitation on the minimal value of the extraction efficiency of the beam. All this formulates rather strict limitation on the beam quality at final radius that depends on the obtained magnetic field map and the characteristics of the particles distribution in the beam beyond the central region. The latter condition requires installation of the beam shaping system at the initial orbits of the cyclotron. In this way phase slit, which consists of two axial posts, is installed in the center. The slit is located at first turn and in dummy dee. Azimuthal position of the device was investigated carefully and corresponds to plane, in which maximal spread of RF phases of ions on their radius takes place. Calculations show that with single phase slit it is possible to separate bunch with RF size not smaller than ~ 8 degree. For selection of micro-bunches it is reasonable to use 2-3 slits installed at different turns. Two regimes of the cyclotron operation were studied – with selection 8-degree and 12-degree bunch in the center. The first one can provide final beam current in agreement with the project requirements (>500 nA). In the second regime extracted beam intensity can exceed $1 \mu\text{A}$. RF acceptance of the central region without phase slits is ~ 50 degree, and beam transmission through the central region is 25%. Axial size of the beam at initial turns is about 5 mm.

The central region provides acceptable beam centering. During acceleration amplitudes of radial betatron oscillations of the beam center of mass are smaller than 2 mm. Introducing first magnetic harmonic near the center with amplitude of 10 Gs leads to decreasing betatron amplitudes to ~ 0.5 mm near the final radius. This fact allows having good radial beam quality there providing this way a high beam extraction efficiency.

Extraction system

Accelerating system consisting of four dees imposes some constraints on the extraction system structure. For example, the extraction elements cannot be positioned in the valleys. For the beam deflection two electrostatic deflectors (ESD) and three passive magnetic channels (MC) are used (Figure 34). A main requirement for the ESDs is rather sufficiently moderate magnitude of the electric field strength there. So, the system is designed in order to have 90-100 kV/cm field strength at the deflectors. The septum thickness of the first ESD is 0.1 mm with the gap between the electrodes of 6 mm. The second ESD has 1-mm septum and gap of 10 mm. Height of the deflectors is 50 mm that allows their placing in the axial gap between the sectors. Every magnetic channel consists of septum (thickness ~ 4 mm) and anti-septum. This structure provides not only field drop

that helps deflecting of the beam, but also creates a positive transverse gradient of the field, which focuses the beam in the radial direction. Parameters of extraction elements are listed in Table 9.

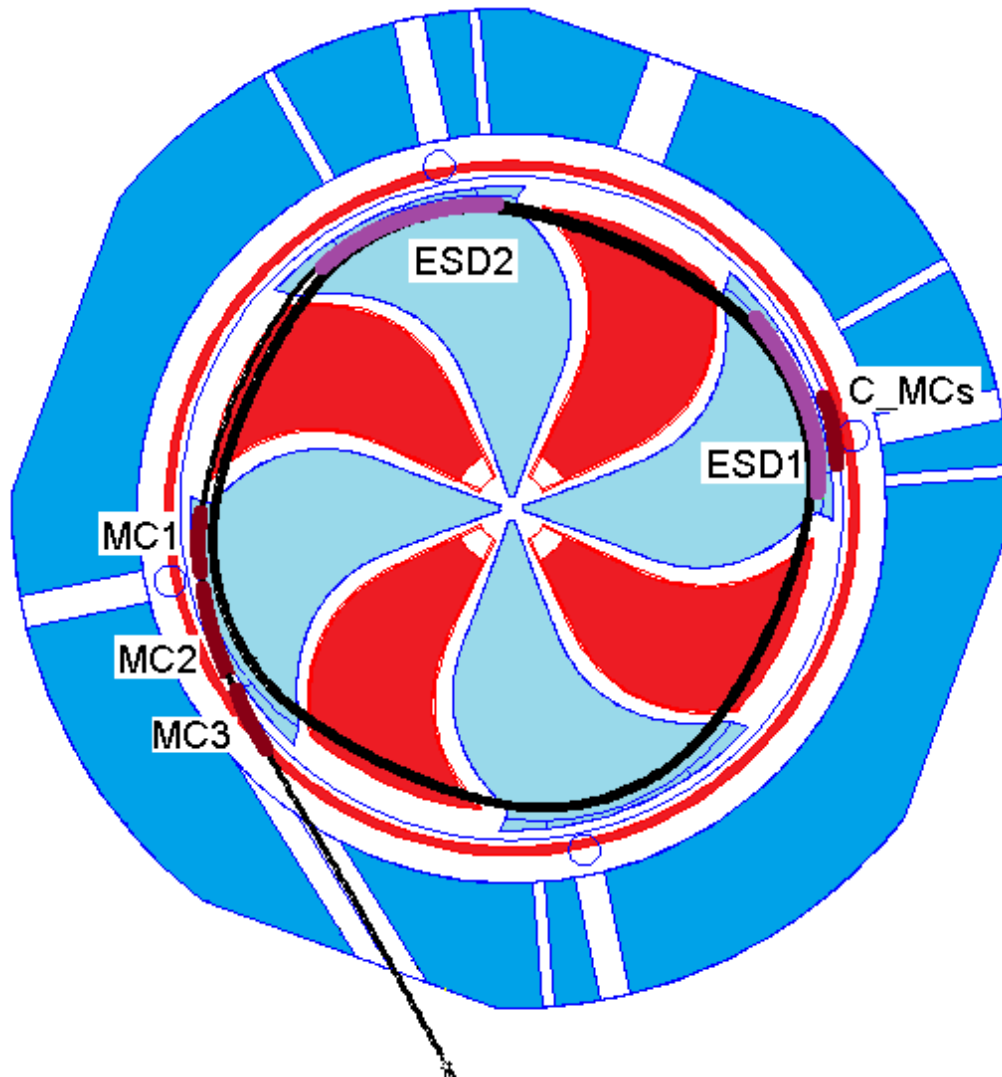


Figure 34. Extraction system of SC230: ESD1 – first electrostatic deflector, ESD2 – second electrostatic deflector, MC1 – first magnetic channel, MC2 – second magnetic channel, MC3 – third magnetic channel, C_MCs – compensator of the first harmonic induced by the magnetic channels.

Table 9. Parameters of extraction elements used in calculations.

Element	Field/Field strength	Field gradient	Length
ESD1	93-97 kV/cm	–	80 cm
ESD2	88-90 kV/cm	–	82 cm
MC1	–1.9 kGs	3 kGs/cm	25 cm
MC2	–1.9 kGs	3 kGs/cm	31 cm
MC3	–0.5 kGs	2 kGs/cm	24 cm

The first magnetic harmonic introduced by magnetic channels is compensated by using a special magnetic element called a compensator (C_MCs), which consists of a single iron bar ($18.6 \times 24 \text{ mm}^2$) that normally should be located just opposite the magnetic channels in azimuth. Since ESD1 already occupies this location, the compensator has to be shifted radially outward of its nominal position. Its shape was optimized for having about the field contribution close to the magnetic channels perturbation in the circulating beam zone but with the opposite sign. The resulting amplitude of first magnetic harmonic on average radius of final orbit is $\sim 3 \text{ Gs}$. The amplitude of second harmonic is $\sim 17 \text{ Gs}$.

A main idea for the extraction system design is deflecting of the extracted beam not too far from the internal beam position upstream the MC1 entrance. This will provide the tolerable beam radial size there. Using magnetic channels with positive field gradients provides rather moderate beam envelopes during extraction process (Figure 34). But radial size of the beam is increasing noticeably from ESD2 to MC1 and is $\sim 13 \text{ mm}$ at the entrance of the channel. Radial aperture of a good field region of MC1 and MC2 is $\sim 10 \text{ mm}$. So, it would be better to have smaller radial size of the beam there. But space between ESD2 and MC1 is occupied by accelerating dee. It is impossible to put some focusing device there. The beam spot at the yoke exit is within $16 \times 12 \text{ mm}^2$ limits.

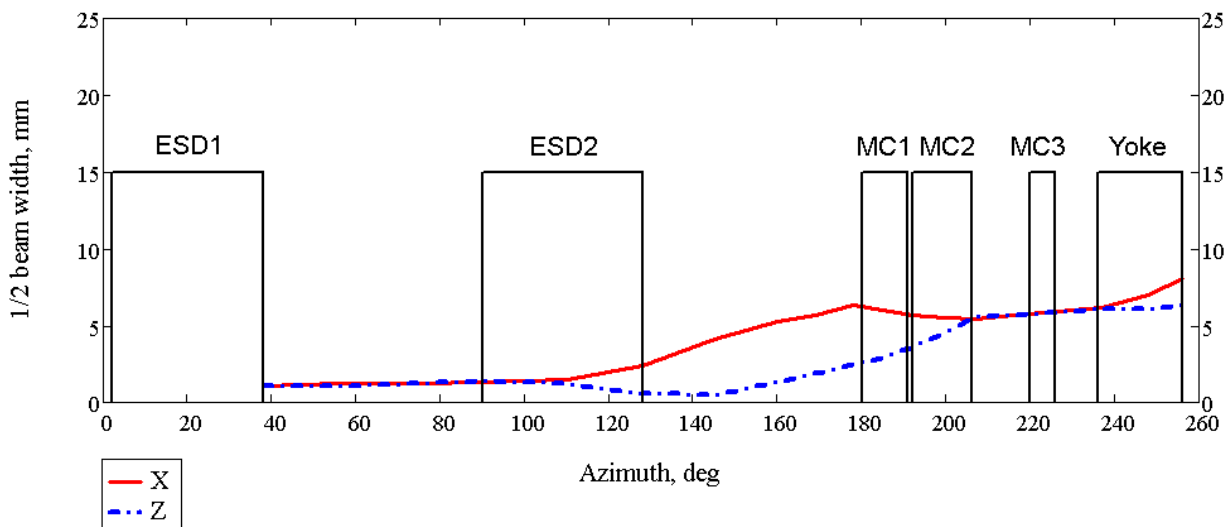


Figure 35. Beam envelopes during extraction (2 standard deviations).

Since size of the beam inside the magnetic channels is large, the beam touches nonlinear field. It results to appearance of tails in the beam emittances. The emittances increase significantly (Figure 36). Introducing of radial focusing in place of ESD2 location can help clearly. For example, ESD2 can be developed with having special shape of electrode to provide radial focusing. Using passive magnetic channel with positive field gradient should provide required effect on the beam. The intensity of the extracted beam is in agreement with the project requirements (Table 10). Multi-turn

extraction from the cyclotron takes place. Contribution of first three turns in total current of the final beam is ~99%.

Introducing of the first harmonic of the magnetic field with small amplitude is useful for boosting of extraction efficiency. For example, utilization of additional first harmonic with amplitude of 5 Gs helps to increase the extraction efficiency of 8-RF degree bunch from 71 to 80%. The effect can be explained by using of first harmonic for small radial shifting of the beam near the final orbit in order to have better matching between ESD1 and the beam.

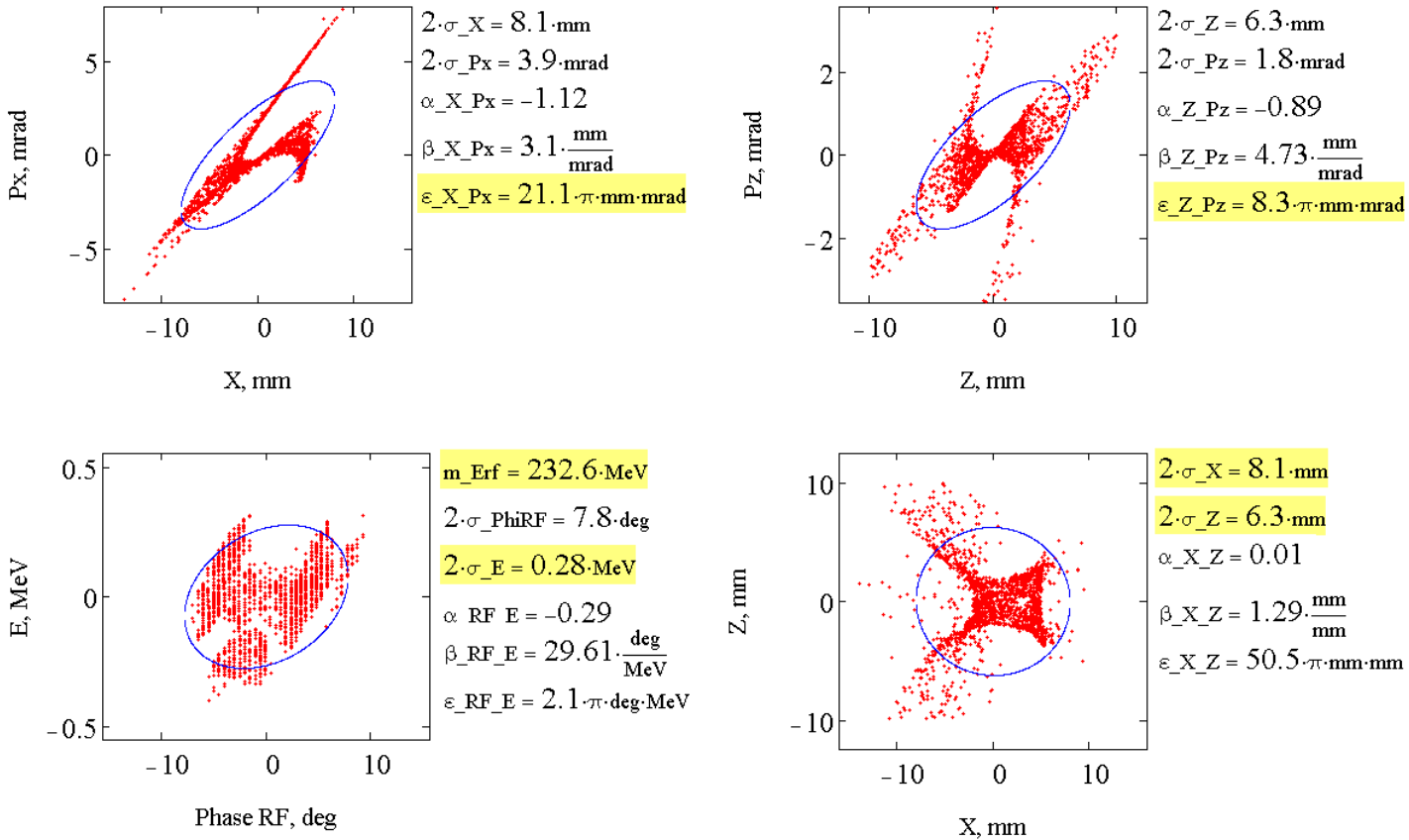


Figure 36. Extracted beam emittances at the yoke exit (12-deg bunch regime).

Table 10. Summary table of characteristics of extracted beam.

BunchRF size after central region, deg	Capture efficiency, %	1 st harmonic amplitude near the final radius, Gs	Beam extraction efficiency, %	Extracted beam current, nA	Horizontal emittance, $\pi \cdot \text{mm} \cdot \text{mrad}$	Axial emittance, $\pi \cdot \text{mm} \cdot \text{mrad}$	Energy spread, %
12	5.6	0	66	1030	21	8	± 0.12
8	2.6	0	71	520	20	7	± 0.11
8	2.6	5	80	580	21	7	± 0.12

Beam dynamics analysis was performed in 3D fields (the only ESD2 field was approximated by an analytical formula with the rest of the field maps estimated by the 3D simulations) from the ion

source to exit of the yoke. The central region provides acceptable beam transmission efficiency and beam centering. The beam extraction efficiency is sufficient, but quality of the final beam is not in compliance with the requirements. Obviously, the beam size downstream the cyclotron can be reduced by using collimators providing of the beam intensity acceptable for treatment. But more intelligent way would be using a passive magnetic channel instead of the second electrostatic deflector. Separation between circulating beam and the extracted beam near ESD2 is ~20 mm that is enough for putting septum of the magnetic channel. Positive gradient of the channel field should provide radial focusing of the beam.

Items that are still waiting to be investigated or designed and simulated:

A device for the beam intensity modulation (axial electrical deflector) in the central region;

Tools for introducing the 1st harmonic of the magnetic field in the central region and near the final radius;

Analysis of effect of resonances on beam quality;

Electrostatic deflector

ESD should be installed in the gap between sectors (50 mm).

The ESD cross section is shown in the Figure 37 . The ESD case is made purely from stainless steel (without gradient).

The radial position of ESD can be tuned in the range ± 5 mm from the optimal position. The gap between septum and high voltage electrode is 6 mm.

The input thickness of the septum is 0.1 mm at height ± 5 mm. The thickness of the septum can be increased from input to output from 0.1 to 1 (2) mm.

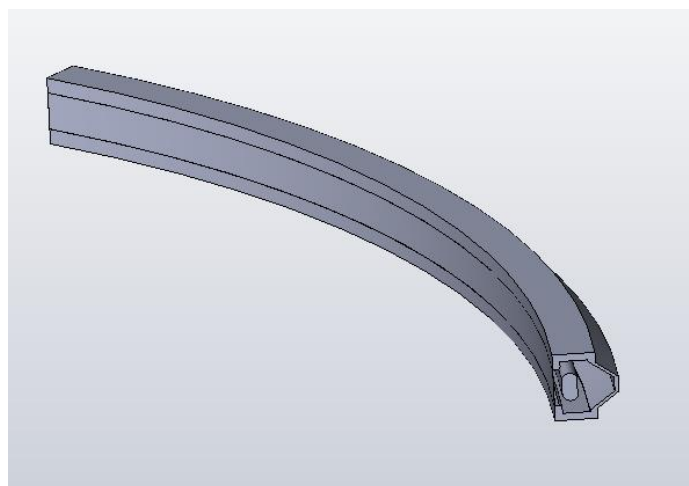
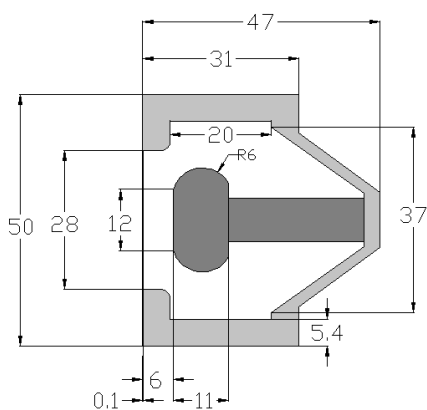
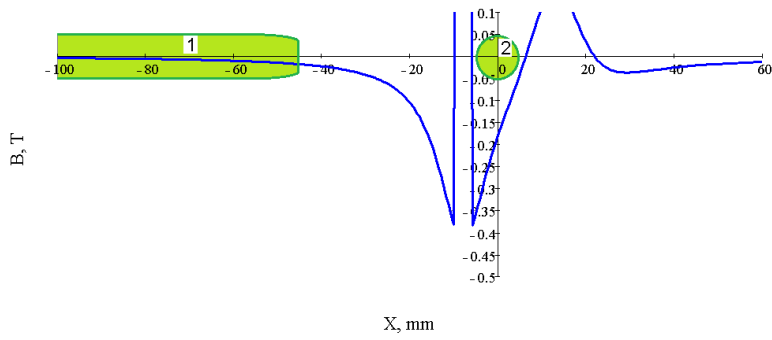
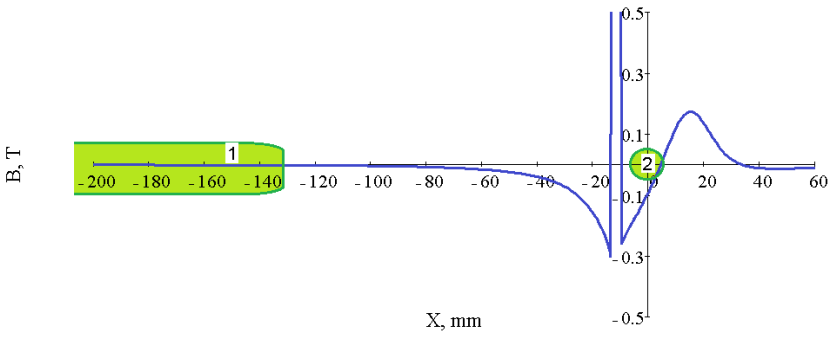


Figure 37. Model of ESD1 that was used for calculation of 3D field. Beam dynamics analysis was performed with this field.

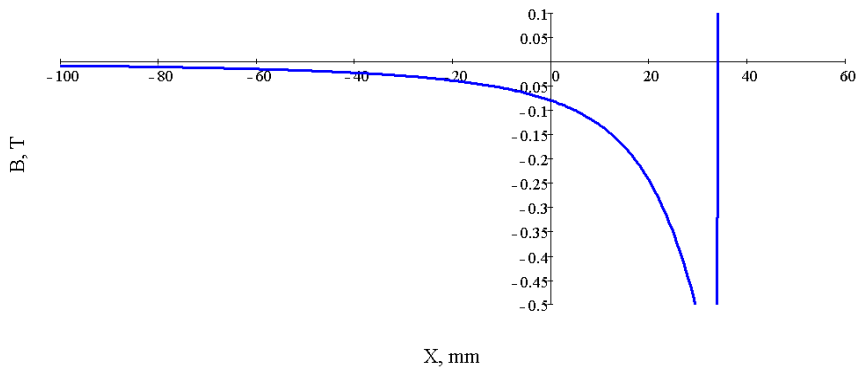
Magnetic channels



a)



b)



c)

Figure 38. Field contribution of MC1 and MC2 (a), MC3 (b), and their compensator (c). Distance between deflected (1) and circulating (2) beam is 45 mm for MC1, 50 mm for MC2, and 130 mm for MC3.

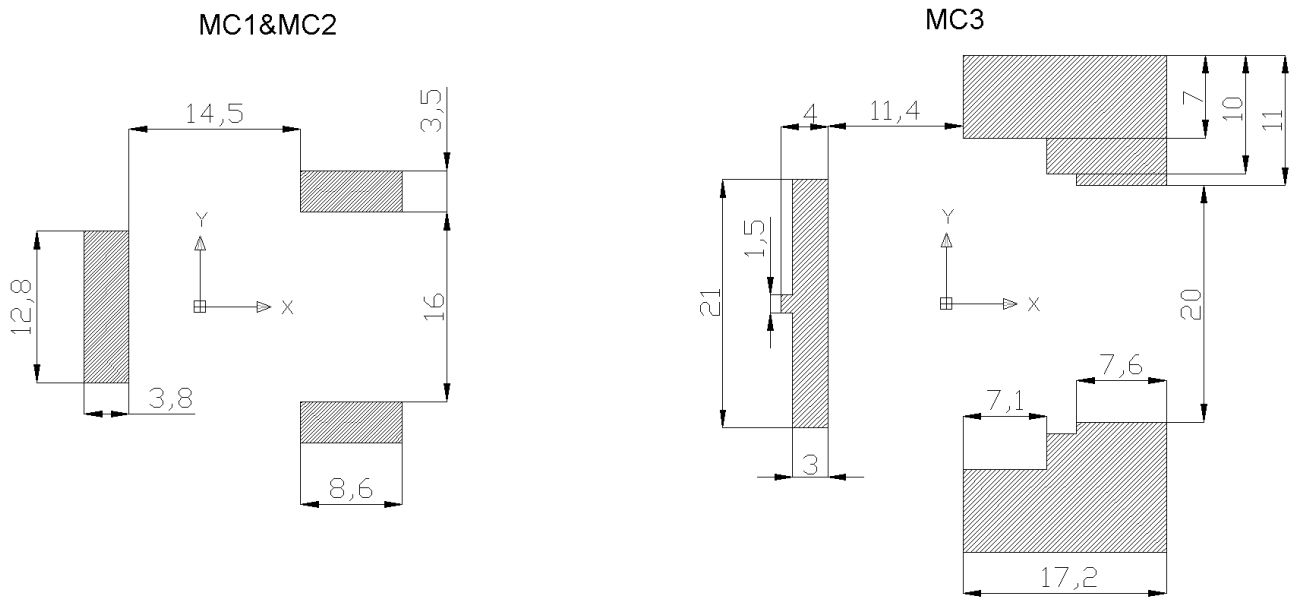


Figure 39. Cross-section of magnetic channels.

Compensator

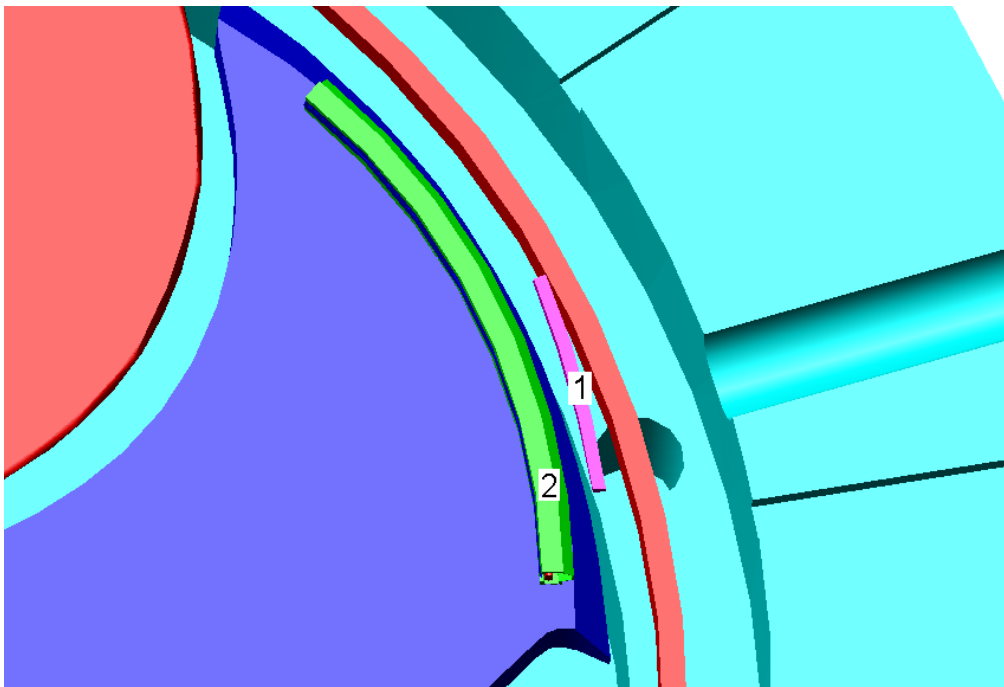


Figure 40. Location of compensator of MCs (1) near ESD1 (2).

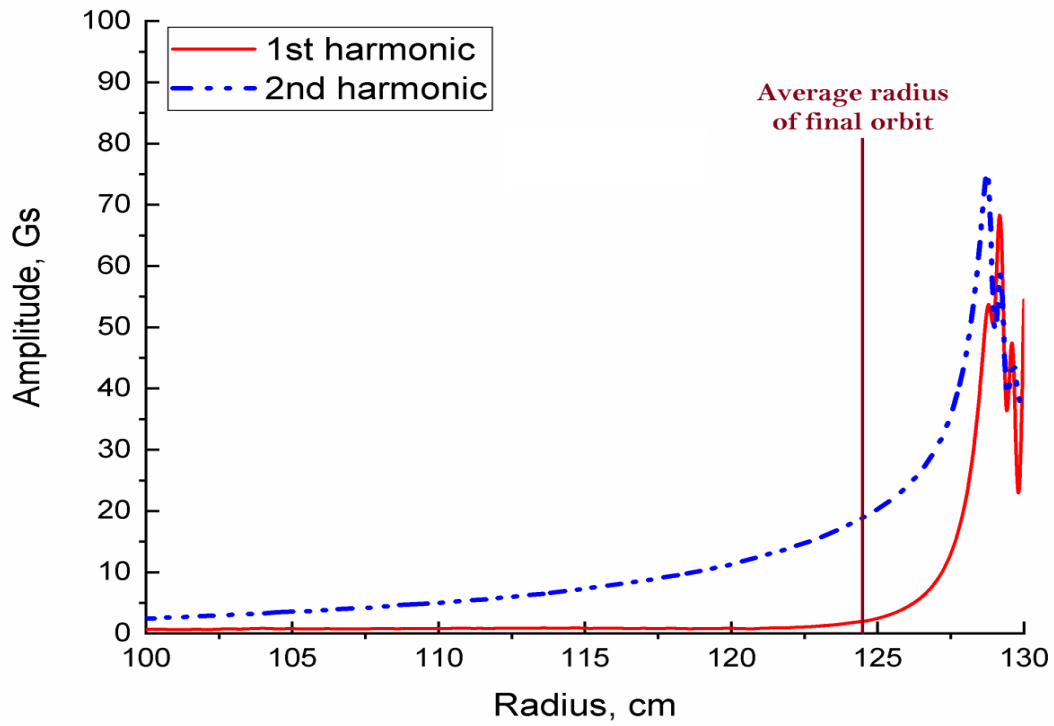


Figure 41. Amplitudes of low harmonics of magnetic field with magnetic channels and compensator.

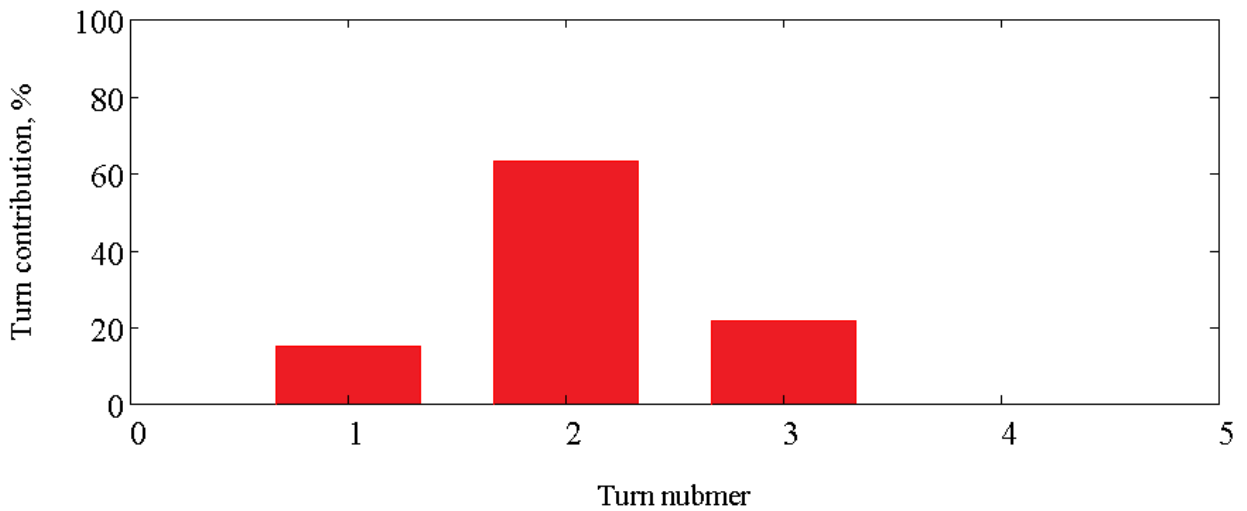


Figure 42. Multi-turn extraction from the cyclotron takes place. Contributions of first three turns are shown in this plot (~99% of total extracted beam).

7. MAGNETIC FIELD MAPPING SYSTEM BASED ON INDUCTIVE COIL.

Motivation

The Hall probe is a more popular method for MFM systems for planar measurements of the cyclotron magnetic fields. This type of magnetometer has a much advantages except the time of mapping. If magnetometer is equipped by only one Hall probe, the time of measurements of a full map 360° , $1^\circ/1\text{cm}$ can reach up to 2-3 days. The time of mapping can be decreased in N times by using N probes. But this way is more complicated in realization.

The alternative method, based on inductive coil gives a much faster MFM system. The time of measurements of a full map 360° , $1^\circ/1\text{cm}$ could be decreased up to 1.5 – 2 hours.

Advantages and disadvantages of inductive coil system

1. Disadvantages – Needs higher investment then the system based on Hall probes since it needs partially different instrumentation and technology then the last one.
2. Advantages – The system is faster and the calibration and errors analysis is much easier then systems based on Hall probe. The system can be easily adapted to measurements at any cyclotrons with about similar dimension magnets.

The similar mapping systems were used for instance in MSU (K500 cyclotron)[12], LNS (Catania – Superconducting cyclotron) [13] or more recently in VECC (Kolkata) [14].

General consideration

The inductive coil method is to measure the field at the center of the magnet with NMR probe and then measure the difference in a field at other points along the magnet radius relative to the center. The coil moves with a uniform velocity along the radius. At the fixed radial positions the system generates start-stop signals to read the coil output. The induced voltage from coil is converted to frequency by a voltage-to-frequency convertor. The number of pulses output by this unit between two coil positions is directly proportional to the field difference. The calibration coefficient could be found by measuring the field at a local maximum in the magnet's field and at the center inside the cyclotron using two NMR or Hall probes.

Proposal of MFM system

It is proposed to build a universal, fast system for measuring magnetic field maps in the median plane of cyclotrons magnets with a pole diameter of about 2 m. The system consists of a horizontal bar settled on the vertical axis driven by a rotation stage. The bar should be made of reinforced carbon-fibre and should sink no more then 0,3 mm. The search coil will be placed on the Teflon (or similar material) cart driven by a motor. This cart will move along the bar with a uniform velocity of

about 20 – 40 cm/sec. When the cart complete its radial motion, the bar rotates to the next angle and the coil returns to its starting position.

The radial steps between datapoints are set by photosensor, placed on a card, and a perforated strip, placed along bar. The accuracy of radial positioning is determined by accuracy of perforation and a uniformity of card velocity. When the photo sensor cross the slit of perforation, the system gets a signal to read the voltage from coil and convert it to frequency by a voltage integrator (Metrolab). The integrator count the number of pulses between two consecutive radial positions. In effect the number of counts at the output of the integrator is a measure of the field difference between two radial positions.

The angular position of each radial scan is determined by an incremental angle encoder accurate to 0.001°.



Figure 43:Metrolab integrator FDI2056 (FLNR has one, it was sent to HIL, Warsaw, as a part of future magnetometer).

As all of the measurements are differential, the absolute value of the field in at least one of the measured points must be known to convert all other differences to the absolute field values. To ensure the proper accuracy it is convenient to use a NMR effect for measurement of the absolute field value in the reference point.



Figure 44: Metrolab NMR teslameter PT2025 (FLNR has one).

However, the reference point in this case has to fulfil the zero gradient requirement of the NMR effect. If the measured field has no points with the gradient equal to 0, the Hall effect can be employed for the reference measurement.



Figure 45:VECC Kolkata cyclotron magnetometer with inductive coil.

Proposed hardware list

1. Voltage Integrator Metrolab FDI2056-1 (in FLNR possession)
2. Rotation Stage
3. Single-axis DC motor controller/driver SMC100CC
4. Horizontal measuring bar with enc.
5. NMR magnetometer or 2 Hall probes, PS, multimeter (in FLNR possession)
6. Search Coil
7. Vertical driving tube
8. Control computer
9. DC motor, controller/driver, electronics, cables, etc.

The proposal MFM system, based on inductive coil, could be manufactured and used in a frame of collaboration at the INFN, JINR, HIL cyclotrons.

The results of measurements will be postprocessed by Matlab CYCLOPS-like code, using a fixed radius approach. The code is already written and verified. The code uses ode23 solver in parallel. The code written in Matlab can be easily and simply modified for specific purposes.

8. VACUUM SYSTEM

SC230 vacuum system can be similar to the vacuum system of SC200 cyclotron and contains cryogenic tank vacuum system, cyclotron main chamber vacuum system, ion source vacuum system.

Possible schema of the main chamber vacuum system is presented in

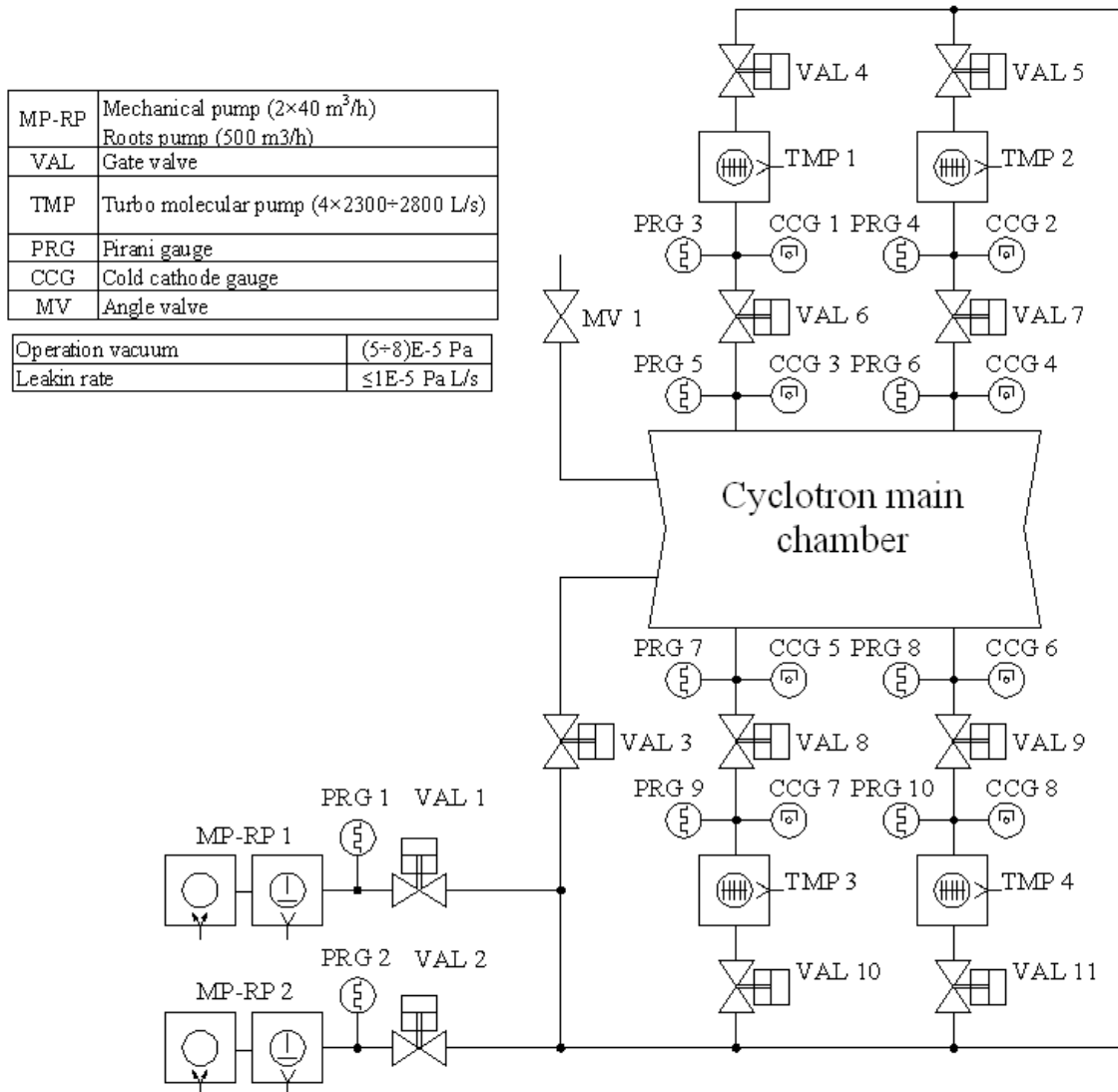


Figure 46.

Figure 46:Cyclotron Main Chamber Vacuum System

CONCLUSION

We chose a low level of the magnetic field in the cyclotron and found out that dimensions of the cyclotron do not increase very much if we use superconducting coils.

Special chamfer on the edge of sector along the particle's trajectory provides isochronism close to the sector edge. Low magnetic field together with high acceleration rate due to 4 cavities and fourth harmonic of acceleration will provide 2-3 mm radial increase of the orbit due to acceleration. As a result we can have efficient extraction with electrostatic deflector.

High acceleration rate reduces tolerances to isochronism. The simplicity of shimming the iron is a great advantage not only for this cyclotron but also for mass production. Computer simulations of the main systems of SC230 cyclotron and beam dynamics have been performed. The technical design of the cyclotron can be finished in 2019.

REFERENCIES

- [1] G.Karamysheva, et al., Present Status of the SC202 Superconducting Cyclotron Project, VIIIth International Particle Accelerator Conference (IPAC 2017), Copenhagen, Denmark, THPVA120.
- [2] <http://www.mevion.com/products/mevion-s250-proton-therapy-system>.
- [3] J. Schippers, R. Dölling, J. Duppich, G. Goitein, M. Jermann, A. Mezger et al., "The SC cyclotron and beam lines of PSI's new proton therapy facility PROSCAN", Nucl. Instr. and Meth., vol.B(261), p.773, 2007.
- [4] D. Vandeplasche et al., Extracted beams from IBA's C235, Proceedings Particle Accelerator Conference, 1997, V.1
- [5] K. Kamakura, Design of a High Temperature Superconducting Magnet for Next Generation Cyclotrons, Doctoral Dissertation, 2019, Japan, http://www.rcnp.osaka-u.ac.jp/~keita/phd_progress/phd_progress.pdf
- [6] <https://www.cst.com>
- [7] <https://www.autodesk.com/products/fusion-360/overview>
- [8] Gen Chen et al., Research and development of RF System for SC200 Cyclotron, 9th International Particle Accelerator Conference, IPAC18, Vancouver, BC, Canada.

- [9] Shiwen.Xu et al., The trajectory simulation and optimization of ion source chimney for SC200 cyclotron, Proceedings of the 17th International Conference on Ion Sources, 2018
- [10] V. L. Smirnov and S. B. Vorozhtsov, SNOP – Beam Dynamics Analysis Code for Compact Cyclotrons, in Proc. of the XXI Russian Accelerator Conference (St. Petersburg, Russia, 2012).
- [11] Xu Shiwen, et. al., Design and test of internal hot-cathode-type PIG ion source for superconducting cyclotron, Nuclear Science and Techniques, 2019.
- [12] G. Bellomo, D.A. Johnson, P. Miller, F.G. Resmini, “Magnetic field mapping of the K-500 cyclotron at M.S.U”, Nuclear Instruments and Methods, Volume 180, Issue 2, Pages 285-304
- [13] P. Gmaj, G. Bellomo, L. Calabretta, D. Rifuggiato, “Final Mapping of the LNS Superconducting Cyclotron”, EPAC 1994, pages 2301-2303
- [14] C. Mallik et al., “Magnetic Field Mapping of Kolkata Superconducting Cyclotron”, Cyclotrons and Their Applications 2007, Eighteenth International Conference, pages 435-437

9. Technical schedule

Scope of work		2019	2020
Stage 1 Development of design documentation of the cyclotron	1.1 Approval of the technical project.	●	
	1.2 Development of working documentation.	●	
	1.3 Development of test program for cyclotron.	●	
Stage 2 Production, control, assembly, acceptance of the cyclotron	2.1 Placing an order for the manufacture of a cyclotron magnetic system.	●	
	2.2 Placing an order for manufacturing a superconducting cyclotron coils	●	
	2.3 Assembly, adjustment and testing of the cyclotron		●
Stage 3 Transportation of the cyclotron to JINR	3.1 Placement an order for cyclotron transportation, coordination and execution of permits and customs documentation		●
	3.2 Transport of the cyclotron from ASIPP to JINR		●

10. Total estimated cost for the project

№№	Source of funding	Total cost (USD)	Costs per years (USD)	
			2019	2020
1.	In-kind contribution from ASIPP in accordance with the JINR-ASIPP cooperation agreement on the development of the Russian-Chinese superconducting cyclotron for an energy of 230 MeV from 10/18/2018	1,278,000	1,278,000	
2.	JINR required expenses for additional equipment and cyclotron transportation to Dubna	2,355,000	2,000,000	355,000
Estimated Total Cost		3,633,000	3,278,000	355,000

11. Equipment summary

Equipment summary To be provided in kind by ASIPP				
DESCRIPTION OF ITEM		Qty	Unit cost (USD)	Amounts (USD)
Yoke	Top Disc	1	45,000	45,000
	Bottom Disc	1	52,000	52,000
	Top Middle Ring	1	60,000	60,000
	Bottom Middle Ring	1	82,000	82,000
	Sectors	8	475,000	475,000
SC Coils	G-Cooler	1	135,000	135,000
	Monitor	1	57,000	57,000
	CTB	1	126,000	126,000
	Coils	2	97,000	194,000
Vacuum system	Vacuum Chamber	1	52,000	52,000
Estimated Total Cost				1,278,000

**Equipment summary
To be purchased by JINR**

DESCRIPTION OF ITEM		Qty	Unit cost (USD)	Amounts (USD)
Vacuum system	Mechanical pump & pump Roots	2	16,000	32,000
	Turbo-molecular pump	4	55,000	220,000
	Gate (VAL6-VAL9)	4	17,000	68,000
	Valve Dy=100 (VAL1, VAL2)	2	3,500	7,000
	Valve Dy=40 (VAL3-VAL5, VAL10, VAL11)	5	1,000	5,000
	Atmospheric valve MV1	1	500	500
	Foreline vacuum sensor PRG1-PRG10	10	500	5,000
	High vacuum sensor	10	1,000	10,000
	Bellows 1500 mm	5	200	1,000
RF system	RF Generator	1	500,000	500,000
	Tuner	1	13,500	13,500
	Feed Through	1	18,000	18,000
	Cavity	1	575,000	575,000
Degrader	Degrader	1	100,000	100,000
Ion Source	Ion Source	1	200,000	200,000
Estimated Total Cost				1,755,000

Annex 1. Estimated cost for cyclotron parts to be purchased by ASIPP



合肥中科离子医学技术装备有限公司

Hefei CAS Ion Medical and Technical Devices Co., Ltd

QUOTATION

To:
No.:
Date: 11 October, 2018

Item	Product	Unit Price (¥)	Remarks
Yoke	Top Disc	300,000	
	Bottom Disc	350,000	
	Top Middle Ring	400,000	
	Bottom Middle Ring	550,000	
	Sector * 8	3,200,000	
SC Coils	G-Cooler	900,000	
	Monitor	380,000	
	CTB	850,000	
	Coils	1,250,000	
RF	Tuner	90,000	
	Feed Through	120,000	
	Cavity	3,850,000	
Vacuum	Vacuum Chamber	350,000	
	Gate Valves	150,000	
Ion Source	Ion Source	1,400,000	
Total		14,140,000	
in US dollars 2,050,000			

Address: 2 Yunfei Road, High-tech District, Hefei, CHINA
 Website: <http://www.hfcim.com/>
 E-mail: info@hfcim.com
 Phone: +86 551-65668736